Two synthetic 18-way outcrossed populations of diploid budding yeast with utility for complex trait dissection

Robert A. Linder[1], Arundhati Majumder[1], Mahul Chakraborty[1], and Anthony Long[1,*]

[1] Department of Ecology and Evolutionary Biology, School of Biological Sciences, University of California, Irvine, Irvine, CA 92697-2525

Short title: *18-way budding yeast synthetic populations*

*Corresponding author:
Anthony Long
Address: Department of Ecology and Evolutionary Biology, University of California, Irvine, Irvine, CA 92697-2525, USA
Phone #: 949 – 824 – 2562
Email: tdlong@uci.edu

Abstract

Advanced generation multi-parent populations (MPPs) are a valuable tool for dissecting complex traits, having more power than GWAS to detect rare variants, and higher resolution than F_2 linkage mapping. To extend the advantages of MPPs in budding yeast, we describe the creation and characterization of two outbred MPPs derived from eighteen genetically diverse founding strains. We carried out *de novo* assemblies of the genomes of the eighteen founder strains, such that virtually all variation segregating between these strains is known and represent those assemblies as Santa Cruz Genome Browser tracks. We discover complex patterns of structural variation segregating amongst the founders, including a large deletion within the vacuolar ATPase *VMA1*, several different deletions within the osmosensor *MSB2*, a series of deletions and insertions at *PRM7* and the adjacent *BSC1*, as well as copy number variation at the dehydrogenase *ALD2*. Resequenced haploid recombinant clones from the two MPPs have a median unrecombined block size of 66kb, demonstrating the population are highly recombined. We pool sequenced the two MPPs to 3270X and 2226X coverage and demonstrate that we can accurately estimate local haplotype frequencies using pooled data. We further down-sampled the poolseq data to ~20-40X and show that local haplotype frequency estimates remain accurate, with median error rate 0.8% and 0.6% at 20X and 40X, respectively. Haplotypes frequencies are estimated much more accurately than SNP frequencies obtained directly from the same data. Deep sequencing of the two populations revealed that ten or more founders are present at a detectable frequency for over 98% of the genome, validating the utility of this resource for the exploration of the role of standing variation in the architecture of complex traits.

Introduction

A complete understanding of the genetic basis of complex traits is a goal shared by many disciplines. Although much progress has been made in dissecting the genetic architecture of complex traits such as adaptation, disease susceptibility, human height, and crop performance, a major fraction of standing variation for most traits has remained recalcitrant to dissection (Manolio *et al.* 2009). This is often referred to as the 'missing' heritability problem. Rapid progress in addressing the missing heritability problem seems most likely in model systems that can be genetically and experimentally manipulated in a controlled setting. In contrast to humans, in model genetic systems variants of subtle effect can be validated via allele replacement experiments.

One of the mainstays of modern genetic mapping studies has been the use of pairwise crosses between genetically diverged founder strains. Large segregating populations can then be used to map phenotype to genotype. This approach, laid out in its modern form for complex traits was initially described by (Lander and Botstein 1989) and reviewed in (Flint and Mott 2001; Mackay 2001; Liti and Louis 2012) has proven to be especially fruitful in budding yeast, such that mapped QTL tend to explain > 70% of the narrow-sense heritability of most traits (Ehrenreich *et al.* 2010; Bloom *et al.* 2013, 2015, 2019; Märtens *et al.* 2016). However, QTL mapping has suffered both from a lack of resolution and a severe under-sampling of the functional variation potentially segregating in natural

65 populations. In this regard, association studies enjoy much finer mapping resolution and
66 sample a larger proportion of the variation present in a natural population (WTCCC 2007;
67 Visscher 2008). However, large-scale association studies are often under-powered to
68 detect rare alleles (Spencer *et al.* 2009), regions that harbor multiple causal sites in weak
69 LD with one another (Pritchard 2001; Thornton *et al.* 2013), rare or poorly tagged
70 structural variants (Hehir-Kwa *et al.* 2016) or variants that are poorly tagged more
71 generally. Furthermore, as GWAS studies grow to include tens of thousands of
72 individuals they can suffer from false positives from population stratification (Berg *et al.*
73 2019) or other experimental block artifacts associated with large scale projects
74 (Sebastiani *et al.* 2011; Chen *et al.* 2017).
75
76 Advanced generation multiparent populations (MPPs) consisting of recombinants derived
77 from several founder individuals have been proposed as a bridge between pairwise
78 linkage mapping and association studies in outbred populations (“The Collaborative
79 Cross, a community resource for the genetic analysis of complex traits” 2004; Macdonald
80 and Long 2007). MPPs are created by crossing several (inbred or isogenic) founder
81 strains to one another in order to maximize diversity, and then intercrossing the resulting
82 population for several additional generations to increase the number of recombination
83 events in the population. In many model systems Recombinant Inbred Lines (RILs) are
84 derived from the MPP via inbreeding. The resulting homozygous RILs are fine-grained
85 mosaics of the original founding strains that have been successfully used to dissect
86 complex traits in *Arabidopsis thaliana* (Kover *et al.* 2009; Huang *et al.* 2011), *Drosophila*
87 *melanogaster* (Macdonald and Long 2007; King *et al.* 2012a, 2012b), *Mus musculus*

(Aylor *et al.* 2011; Threadgill and Churchill 2012), *Saccharomyces cerevisiae* (Cubillos *et al.* 2013), *Zea mays* (McMullen *et al.* 2009), *Caenorhabditis elegans* (Noble *et al.* 2019), and several other systems (de Koning and McIntyre 2017). MPP RILs are a powerful resource for dissecting complex traits due to increased mapping resolution relative to F2 populations and increased natural variation sampled by the founders. Furthermore, unlike association studies, both rare alleles of large effect segregating among the founders as well as allelic heterogeneity can be detected in MPP RILs (Long *et al.* 2014). Although the majority of studies to date have studied RILs derived from MPPs, it is possible to dispense with the creation and maintenance of RILs and sample the MPP directly (Mott *et al.* 2000; Macdonald and Long 2007), and indeed early MPP efforts did not employ RILs.

Despite the clear advantages of MPPs, only a single MPP has been described in budding yeast (Cubillos *et al.* 2013), which is surprising as this species is ideally suited in many other ways for the dissection of complex traits. Large population sizes can be maintained in a controlled environment and a few rounds of meiosis results in recombination events spaced at near genic resolution. The potential of MPPs in budding yeast was demonstrated by Cubillos et al., who crossed four genetically highly diverged strains and intercrossed the resulting population for twelve generations to generate a highly recombined population that has been shown to be capable of mapping complex traits to high resolution (Cubillos *et al.* 2013, 2017). In order to expand the potential of budding yeast to contribute to our understanding of complex traits we have developed two large, highly outbred populations of budding yeast derived from a cross of 18 genetically

diverged founders. Like previous work, populations were intercrossed for 12 generations to produce highly recombined mosaic populations that capture a large amount of the standing variation present in *S. cerevisiae*. Here we describe the derivation of the founders that allows the 18-way cross to be carried out, *de novo* PacBio assemblies of each founder such that all variation segregating in the population is known, and the characterization of ten haploid recombinant clones from each population to estimate the size distribution of haplotype blocks in the MPPs. We further carry out deep short read resequencing of the MPPs, estimate founder haplotype frequencies as a function of location in the genome, and show that at Illumina sequencing coverages as low as ~20X-40X haplotype frequencies can be accurately estimated. The MPPs and tools we derive have great utility for dissecting complex traits in yeast.

Materials and Methods

Strains and media

All yeast strains used in this study came from heterothallic, haploid derivatives of a subset of the SGRP yeast strain collection kindly provided by Gianni Liti (Cubillos *et al.* 2009). A list of strains used, relevant genotypes (before and after our modifications), and their geographical origins is shown in Table 1. Additionally, two mate-type testing yeast strains were used (kindly provided by Ian Ehrenreich) that are selectively killed by the presence of either *Mat a* or *Mat α* haploids, but not by diploids. For propagating plasmids, *Escherichia coli* strain DH5α was used according to the manufacturer's recommendations (Invitrogen). Bacterial transformants were selected on LB agar, supplemented with 100ug/mL ampicillin ('LBamp') (Fisher). Nonselective media for growth and maintenance

of all yeast strains included rich media consisting of 1% yeast extract, 2% peptone, and 2% dextrose ('YPD') (Fisher). For solid media, 2% agar was added. Additionally, media consisting of 1% yeast extract, 2% peptone, 2% glycerol and 2.5% ethanol ('YPEG') was used to prevent the growth of *petite* mutants. For selecting yeast transformants, when *Ura3MX* was the marker, synthetic complete drop-out uracil (Sc -Ura) plates were used (Sunrise Scientific). When *KanMX*, *HphMX*, or *NatMX* were the markers used, transformants were selected on YPD plates supplemented with 200ug/mL of G418, 300ug/mL of Hygromycin B ('hyg'), or 100ug/mL nourseothricin sulfate ('cloNAT'), respectively. For counterselection of yeast that lost the *Ura3MX* marker, synthetic complete media supplemented with 1mg/mL 5-FOA was used ('5-FOA'). Two types of sporulation media were used in this study. Type 1 consisted of 1% potassium acetate, 0.1% yeast extract, and 0.05% dextrose ('PYD') to which ampicillin was added to a final concentration of 50ug/mL, while type 2 consisted of 1% potassium acetate and a 1X dilution of a 10X amino acid stock (composed of 3.7g of CSM -lysine (Sunrise Scientific) supplemented w/10mL of 10mg/mL lysine in 1L total volume), pH adjusted to 7 ('PA7'). Just before use, ampicillin was added to PA7 to a final concentration of 100ug/mL.

Modification of 24 haploid budding yeast strains to create founders for the synthetic population

The strains used in this study were modified by generating clean deletions of the *HO* gene to recover the *HphMX* marker, followed by replacement of a pseudogene, *YCR043C*, which is closely linked to the mating type locus, with either a *NatMX* cassette in *Mat a*

haploids or a *HphMX* cassette in *Mat α* haploids. This manipulation was carried out to enable high-throughput selection of diploids.

The *HphMX* marker in *HO* was recovered via transformation with a URA3 cassette flanked with direct repeats and selection on URA- plates followed by selection on 5-FOA plates to recover URA3. The URA3 cassette was assembled from four fragments: a pBluescript II KS(+) backbone linearized with EcoRV and gel purified (for propagation in *Escherichia coli*), the *URA3* gene from *Candida albicans* with flanking 500bp direct repeats from *Aschbya gossypii* (pAG61, addgene #35129), and a 450bp region directly upstream of the *HO* gene, and a 390bp region directly downstream of the *HO* gene. Primers pAG61_HO-F/R were used to amplify *URA3* and the flanking direct repeats, while primers HO-US F/R and HO-DS F/R were used to amplify the regions flanking the *HO* gene from strain DBVPG6765. Primers used in this study are listed in Table S1 and included overhangs to allow for HiFi assembly. The four fragments were assembled using the NEB HiFi Assembly Master Mix according to the manufacturer's recommendations (NEB), transformed into chemically competent DH5α (Invitrogen), and recovered on LB Amp plates. Recovered URA plasmid cassettes with *HO* flanking sequences were PCR amplified from the plasmid template using primers HO-US-F and HO-DS-R, transformed into all 24 haploid strains using a standard lithium acetate protocol, and plated onto Sc -Ura plates. Single colonies were re-streaked onto Sc -Ura (X2), final colonies were tested for the presence of the *KanMX4* marker and absence of *HphMX4* marker via *G418* and *hyg* plating respectively. O/N cultures of successfully knocked-out transformants were spread onto 5-FOA plates and grown for 2d at 30°C in order to select for cells that had

179 'popped out' the *Ura3* cassette. Single colonies were re-streaked onto 5-FOA plates (2X).
180 DNA was extracted (adapted from CSH handbook, p. 116) from the resulting colonies
181 and DNA amplicons spanning the *HO* locus were obtained and Sanger sequenced to
182 confirm the clean deletion of the *HO* gene.
183
184 To delete *YGR043C* in the 24 newly generated haploid *hoΔ Ura3::KanMX4* strains, oligos
185 were ordered from IDT that amplify the entire MX4 cassette, including the promoter and
186 terminator regions, and were tailed with 100 bases of homology to the regions
187 immediately upstream and downstream of the *YGR043C* CDS. Either pAG32 (addgene
188 #35122) or pAG25 (addgene #35121) were used as a template to generate knock-out
189 constructs that incorporate the *HphMX4* or *NatMX4* cassettes, respectively. PCR
190 reactions were cleaned up to remove unamplified circular plasmid template by gel
191 extraction followed by digestion with DpnI and a PCR cleanup reaction (Qiagen PCR
192 Purification kit). *Mat a* yeast were then transformed with the *cloNAT* resistance cassette,
193 while *Mat α* yeast were transformed with the *hyg* resistance cassette using the standard
194 lithium acetate protocol and selecting on YPD supplemented with cloNAT and G418 or
195 hyg and G418, respectively. This double selection with G418 was done to ensure that
196 cassette swapping had not occurred. To ensure *YGR043C* had been correctly replaced
197 in each strain, the region was amplified and Sanger sequenced. All 24 newly generated
198 strains were checked again for *HO* deletion using the HO-big-flank-F/R primers. The
199 strains were also checked to ensure they had maintained the correct barcodes originally
200 inserted in Cubillos et al throughout all the manipulation steps by amplifying the barcodes
201 using the barcode-check-F/R primer pair and Sanger sequencing the amplicons using the

202 M13(-47)F primer. As a final check, all 24 haploid strains were streaked onto YPD
203 supplemented with hyg and cloNAT to ensure that none of the strains could grow on both
204 antibiotics.

205

206 **Table 1.** An overview of the strains used in this study.

ADL*	NCYC	Isolate	Origin	Original genotype	Modified genotype**
A1	3597	DBVPG6765	Europe	*Mat a, ho::HygMX,ura3::KanMX-Barcode*	*Mat a,* ***hoΔ****, ura3::KanMX-Barcode,* ***ygr043C::NatMX***
A2	3600	DBVPG6044	West Africa; wine	*Mat a, ho::HygMX,ura3::KanMX-Barcode*	*Mat a,* ***hoΔ****, ura3::KanMX-Barcode,* ***ygr043C::NatMX***
A3	3607	YPS128	USA; soil beneath Quercus alba	*Mat a, ho::HygMX,ura3::KanMX-Barcode*	*Mat a,* ***hoΔ****, ura3::KanMX-Barcode,* ***ygr043C::NatMX***
A4	3605	Y12	Japan; sake	*Mat a, ho::HygMX,ura3::KanMX-Barcode*	*Mat a,* ***hoΔ****, ura3::KanMX-Barcode,* ***ygr043C::NatMX***
A5	3586	YIIc17_E5	France; wine	*Mat a, ho::HygMX,ura3::KanMX-Barcode*	*Mat a,* ***hoΔ****, ura3::KanMX-Barcode,* ***ygr043C::NatMX***
A6	3591	BC187	USA; wine	*Mat a, ho::HygMX,ura3::KanMX-Barcode*	*Mat a,* ***hoΔ****, ura3::KanMX-Barcode,* ***ygr043C::NatMX***
A7	3590	SK1	USA; soil	*Mat a, ho::HygMX,ura3::KanMX-Barcode*	*Mat a,* ***hoΔ****, ura3::KanMX-Barcode,* ***ygr043C::NatMX***
A8	3598	L_1374	Chile; wine	*Mat a, ho::HygMX,ura3::KanMX-Barcode*	*Mat a,* ***hoΔ****, ura3::KanMX-Barcode,* ***ygr043C::NatMX***
A9	3602	UWOPS03_461_4	Malaysia; nectar, Bertram palm	*Mat a, ho::HygMX,ura3::KanMX-Barcode*	*Mat a,* ***hoΔ****, ura3::KanMX-Barcode,* ***ygr043C::NatMX***
A10***	3604	UWOPS05_227_2	Malaysia; stingless bee, near Bertram palm	*Mat a, ho::HygMX,ura3::KanMX-Barcode*	*Mat a,* ***hoΔ****, ura3::KanMX-Barcode,* ***ygr043C::NatMX***
A11	3592	YJM978	Italy; vagina, clinical isolate	*Mat a, ho::HygMX,ura3::KanMX-Barcode*	*Mat a,* ***hoΔ****, ura3::KanMX-Barcode,* ***ygr043C::NatMX***

A12	3594	YJM975	Italy; vagina, clinical isolate	*Mat a, ho::HygMX,ura3::KanMX-Barcode*	*Mat a,* ***hoΔ,*** *ura3::KanMX-Barcode,* ***ygr043C::NatMX***
B1	3622	DBVPG6765	Europe	*Mat α, ho::HygMX,ura3::KanMX-Barcode*	*Mat α,* ***hoΔ,*** *ura3::KanMX-Barcode,* ***ygr043C::HygMX***
B2	3625	DBVPG6044	West Africa; wine	*Mat α, ho::HygMX,ura3::KanMX-Barcode*	*Mat α,* ***hoΔ,*** *ura3::KanMX-Barcode,* ***ygr043C::HygMX***
B3	3632	YPS128	USA; soil beneath Quercus alba	*Mat α, ho::HygMX,ura3::KanMX-Barcode*	*Mat α,* ***hoΔ,*** *ura3::KanMX-Barcode,* ***ygr043C::HygMX***
B4	3630	Y12	Japan; sake	*Mat α, ho::HygMX,ura3::KanMX-Barcode*	*Mat α,* ***hoΔ,*** *ura3::KanMX-Barcode,* ***ygr043C::HygMX***
B5	3611	273614N	UK; fecal sample, clinical isolate	*Mat α, ho::HygMX,ura3::KanMX-Barcode*	*Mat α,* ***hoΔ,*** *ura3::KanMX-Barcode,* ***ygr043C::HygMX***
B6	3631	YPS606	USA; bark of *Quercus rubra*	*Mat α, ho::HygMX,ura3::KanMX-Barcode*	*Mat α,* ***hoΔ,*** *ura3::KanMX-Barcode,* ***ygr043C::HygMX***
B7	3624	L_1528	Chile; wine	*Mat α, ho::HygMX,ura3::KanMX-Barcode*	*Mat α,* ***hoΔ,*** *ura3::KanMX-Barcode,* ***ygr043C::HygMX***
B8	3614	UWOPS83_787_3	Bahamas; fruit, *Opuntia megacantha*	*Mat α, ho::HygMX,ura3::KanMX-Barcode*	*Mat α,* ***hoΔ,*** *ura3::KanMX-Barcode,* ***ygr043C::HygMX***
B9	3609	UWOPS87_2421	USA; cladode, *Opuntia megacantha*	*Mat α, ho::HygMX,ura3::KanMX-Barcode*	*Mat α,* ***hoΔ,*** *ura3::KanMX-Barcode,* ***ygr043C::HygMX***
B10***	3628	UWOPS05_217_3	Malaysia; nectar, Bertram palm	*Mat α, ho::HygMX,ura3::KanMX-Barcode*	*Mat α,* ***hoΔ,*** *ura3::KanMX-Barcode,* ***ygr043C::HygMX***
B11	3618	YJM981	Italy; vagina, clinical isolate	*Mat α, ho::HygMX,ura3::KanMX-Barcode*	*Mat α,* ***hoΔ,*** *ura3::KanMX-Barcode,* ***ygr043C::HygMX***
B12	3613	Y55	France; grape	*Mat α, ho::HygMX,ura3::KanMX-Barcode*	*Mat α,* ***hoΔ,*** *ura3::KanMX-Barcode,* ***ygr043C::HygMX***

* These are the abbreviated names used throughout this manuscript. Note that all A strains are Mat a, and all B strains Mat α.

** Bold text indicates changes made from the original strain genotypes.

*** These two strains were excluded from subsequent experiments as they mate poorly with the other strains.

18-way crossing scheme, version 1

A full diallele cross of eleven *Mat a* and eleven *Mat α* strains (excluding strains A10 and B10) was carried out (with four strains in common). A schematic of the mating scheme is shown in Figure 1A, while Table 1 lists the strains used in this study. Strains A1-A5 and A6-A12 (excluding A10) were struck in horizontal rows onto two YPD plates each (total of 4 YPD plates), then strains B1-B5 and B6-B12 (excluding B10) were each struck in vertical rows onto two of the YPD plates such that each 'B' strains intersected with each 'A' strains. All 121 pairwise combinations of the 'A' and 'B' strains were thus represented across the four YPD mating plates. Mating occurred O/N at 30°C after which diploids were selected by replica plating onto YPD plates with hyg and cloNAT. A single colony from each of the 121 crosses was then incubated O/N in YPD with hyg and cloNAT at 30°C at 180RPM. An equal volume of each culture and 30% glycerol was used to make frozen stock that was then archived at -80°C. An equal volume from each diploid culture was then combined to make the 18-way population, which was washed twice with PYD + amp then split into two 1L flasks with 200mL total PYD + amp each. Sporulation was carried out for 5d *en mass* at 30°C at 180RPM to complete the first round of out-crossing.

Additional outcrossing in the 18-way cross, version 1

Eleven additional cycles of mass sporulation followed by random mating were carried out for a total of twelve rounds of outcrossing for both replicates (Table S3). After sporulation, 50mL of culture was spun down at 2000g for 2m and resuspended in 1mL of Y-PER. Samples were transferred to a 1.5mL centrifuge tube and vortexed. Cells were washed twice and resuspended in 500uL of ddH_2O with 5uL of 5U/uL zymolyase. The tubes were

shaken vigorously in the Geno Grinder 2000 at 750 shakes/minute for 45m. 500uL of 400um silica beads were then added to the samples, which were again put in the Geno Grinder for 5m at 1500 shakes/minute. The supernatant was transferred to a fresh 1.5mL centrifuge tube, washed once in YPD, resuspended in 500uL of YPD, and transferred into 50mL of YPD in a 1L flask. Mating was carried out O/N at 30°C at 40RPM. The next day, mated cells were harvested, transferred to YPD with cloNAT, hyg, and amp, and incubated O/N at 30°C at 180RPM. The next day, 7mL from the O/N culture was used to make glycerol stock while 5mL was harvested, washed twice, and resuspended in 200mL of PYD + amp. Sporulation was carried out for 5d at 30°C at 180RPM (see Table S2). If the experiment had to be paused, 5mL of glycerol stock from the most recently completed cycle was used to begin the next cycle of sporulation.

18-way crossing scheme, version 2

A full diallele cross of the same eleven *Mat a* and eleven *Mat α* founder strains used to create 18F12v1 was again carried out. To initiate this process, an equal volume from cultures containing each *Mat a* founder strain were mixed with each *Mat α* founder strain in all 121 possible pairwise combinations in 24-well deep-well plates (hereafter '24DWP') in a total volume of 1mL of YPD (no ampicillin added) (see Note S1). Mating was carried out in liquid culture for 4-5h at 30°C at 50RPM, after which mating was verified by checking for the presence of zygotes and/or shmooing under a microscope. At this point, 1mL of YPD supplemented with 200ug/mL cloNAT and 600ug/mL hyg was added to each culture (the final concentrations of cloNAT and hyg were 100ug/mL and 300ug/mL, respectively) to select for successfully mated diploids and incubated O/N at 200RPM at

30°C. After O/N selection, 140uL from each culture was combined w/140uL of 30% glycerol to make frozen stock of each cross. The remaining cultures were harvested at 3000 RPM for 5m and the pellets were washed then resuspended in 4mL of PA7 + amp. Sporulation was carried out for 6d at 30°C at 275 RPM in the 24DWPs.

All 121 sporulating cultures were checked using a microscope to determine the amount of sporulation that occurred; cultures were graded on a scale of 0-5 with 0 being no sporulation and 5 being almost complete sporulation. Crosses that did not sporulate were excluded from subsequent steps (see Table S2). After checking for sporulation, cultures were harvested, washed, then resuspended in 500uL of spore isolation solution (hereafter 'SIS': 25U zymolyase + 10mM DTT + 50mM EDTA + 100mM Tris-HCl, pH 7.2 up to 500uL) and incubated for 1h at 30°C at 250 RPM to spheroplast cells. Cultures were then harvested and resuspended in 1% Tween 20 to selectively lyse unsporulated cells. Following this, cultures were again harvested and resuspended in 500uL of spore dispersal solution (hereafter 'SDS': 1mg lysozyme + 5U zymolyase + 1% Triton X-100 + 2% dextrose + 100mM PBS, pH 7.2 up to 500uL). Cultures were transferred to Eppendorf tubes with 500uL of 400um beads and bead milled using a Geno Grinder 2000 at 1500 strokes per minute for 5m to break up tetrads after which all cultures were placed at 4°C O/N. The next day, all tubes were vortexed at high speed for 30s, the supernatant was transferred to a 24DWP, 500uL of 100mM PBS, pH 7.2 was added back to the beads, followed by vortexing for 30s and transferring to the same wells of a 24DWP to maximize recovery of spores from the beads. Cultures were washed once in PBS, then resuspended in 500uL of 100mM PBS, pH 7.2 and 100uL was transferred to a 96-well

clear plate to measure the OD630 of each culture in duplicate using a BioTek Synergy HT plate reader. OD630 measurements were then used to normalize the density of spores from each cross that were pooled together (see Note S2). The spore pool was washed twice with 5mL of YPD, then resuspended in 12.5mL of YPD. This culture was split in half and transferred to two 250mL flasks, each with 6.25mL of YPD, to establish two replicate populations. Mating was carried out O/N at 30°C with gentle shaking at 40 RPM. The next day, 12.5mL of YPDach (with a 2x mix of ampicillin, cloNAT, and hyg) was added to each culture to select for diploids. Cultures were incubated O/N at 200 RPM at 30°C. This established replicate F_2 populations of the 18-way cross, version 2 (hereafter '18F2v2'). The following day, 7mL of the replicate populations were frozen down at -80°C with an equal volume of 30% glycerol. The remaining volume was spun down and used to initiate a second round of outcrossing.

Additional outcrossing in the 18-way cross, version 2

Eleven additional cycles of mass sporulation followed by random mating were carried out for a total of twelve rounds of outcrossing for both replicates. As replicate 2 was treated differently during a couple of cycles, replicate 1 was the population chosen for subsequent analyses and, as such, will be the only replicate of version 2 described further. Each cycle consisted of 3-6d of sporulation after which diploids were randomly mated for 3-4h. This was followed by an O/N selection step in YPDach to enrich for mated diploids. After selection, an aliquot of each population was frozen down at -80°C with the remaining culture used to initiate the next cycle of outcrossing. Table S3 enumerates the days of sporulation for each cycle as well as additional details regarding the culturing conditions

for both versions of the 18-way population. After each round of sporulation, cultures were processed as detailed above with the following modifications: 5mL of SIS, 10mL of 1% Tween 20, and 5mL of SDS were used to kill vegetative cells. Tetrads were disrupted by bead milling at 1500 strokes/minute using the Geno Grinder 2000 for 25-45m. The contents of the tubes were mixed thoroughly with a pipette to ensure maximal recovery of cells from the bead slurry. The supernatant was then transferred to 50mL Falcon tubes, after which 500uL of YPDa was added back to the tubes, which were then vortexed at the highest setting briefly. The supernatant was transferred to the same 50mL Falcon tube. Cultures were harvested, washed, then resuspended in 5mL of YPDa. At this point, cells were carefully mixed by pipetting and then transferred to a 250mL Erlenmeyer flask with 7.5mL of YPDa. Spores were mated for 3-4h at 30°C at 40RPM, after which the presence of shmoos and/or zygotes was checked under the microscope. 12.5mL of YPDach was added to the mated cells, which were incubated O/N at 200RPM at 30°C. The next day, cells were transferred to 50mL Falcon tubes, 7mL of culture was mixed with an equal volume of 30% glycerol to make frozen stock, while the rest of the culture was spun down at 3000RPM for 5m. Cultures were washed twice, resuspended in 25mL of PA7, then transferred to a 250mL flask with 50uL of 100mg/mL ampicillin and sporulated at 30°C at 275RPM to initiate the next cycle of outcrossing. Following the twelfth cycle of sporulation followed by random mating, cells were transferred to 1L flasks with 187.5mL of YPDach and incubated O/N at 30°C at 200RPM. The following day, all 200mL of culture was mixed with an equal volume of 40% glycerol and frozen down at -80°C in a combination of 2mL cryotubes and 15mL Falcon tubes.

Table 2. Assembly statistics for the 18 sequenced founder strains.

Strain	Assembly size (Mb)	Assembly N50 (kb)	Assembly QV	Assembly BUSCO (complete)	Total PacBio data (Mb)	PacBio read N50 (kb)	Total Illumina data (Mb)	Type of Illumina reads	x PacBio coverage	x Illumina coverage
A5	12.13	757	48.8	0.990	737	11.10	3,396	PE100	61.4	283.0
A6	11.98	913	46.6	0.986	620	11.68	4,079	PE150	51.7	340.0
A7	12.62	901	66.2	0.990	3,979	5.97	2,775	PE100	331.6	231.3
A8	12.03	917	55.5	0.993	622	11.79	3,420	PE100	51.9	285.0
A9	12.53	571	53.0	0.993	5,845	5.10	2,769	PE100	487.1	230.7
A11	12.10	702	49.3	0.986	644	12.03	2,758	PE100	53.7	229.8
A12	12.00	795	45.5	0.993	613	11.83	3,563	PE100	51.1	296.9
B5	12.32	738	46.5	0.990	741	10.97	3,861	PE100	61.7	321.8
B6	12.10	772	44.9	0.990	401	11.67	2,906	PE100	33.4	242.2
B7	11.91	765	39.5	0.986	719	11.79	4,266	PE100	59.9	355.5
B8	11.99	802	66.0	0.990	741	12.00	3,054	PE100	61.8	254.5
B9	12.40	856	54.6	0.993	1,083	12.05	3,419	PE100	90.2	284.9
B11	12.12	789	55.0	0.990	765	12.13	2,236	PE100	63.8	186.3
B12	12.04	790	48.7	0.986	804	10.79	3,930	PE100	67.0	327.5
AB1	12.35	901	47.9	0.993	3,315	5.84	3,509	PE150	276.3	292.4
AB2	12.83	741	66.2	0.990	5,230	4.77	4,230	PE150	435.8	352.5
AB3	12.44	809	55.8	0.990	3,254	6.21	3,891	PE150	271.2	324.2
AB4	12.32	800	55.7	0.990	4,649	6.43	4,490	PE150	387.4	374.2

*Cells highlighted in blue represent founder strains that were previously sequenced using PacBio technology in (Yue *et al.* 2017)

Whole genome sequencing of the haploid founder strains

All 18 founder strains were sequenced using a combination of PacBio long read and Illumina short read technology. PacBio sequencing data was available from a previous study for 6 of the 18 strains (founder AB1-AB4, A7, and A9) (Yue *et al.* 2017), which was downloaded and reassembled using our pipeline so that all assemblies are directly comparable. The remaining strains were struck out onto YPD plates for 3d at 30°C, after which a single colony was inoculated into 50mL of YPDamp and incubated at 30°C at 200RPM O/N. DNA was extracted using the Qiagen G-tip DNA extraction kit. Purified

341 genomic DNA was sheared using 24-gauge blunt needles. The resulting sheared gDNA
342 samples were quality checked by a FIGE run at 134V O/N and concentrations were
343 measured using Qubit. Sample were considered acceptable if the majority of gDNA was
344 sheared to between 20kb and 100kb. In our hands carefully controlling the gDNA size
345 distribution results in longer N50 PacBio reads which gives better *de novo* assemblies
346 with less data. SMRTbell libraries were prepared and sequenced at the UCI Genomics
347 High Throughput Facility using a PacBio RSII machine. The details of PacBio library
348 creation for the purpose of *de novo* genome assembly are described in (Chakraborty *et*
349 *al.* 2016). The average per-site coverage of the six previously sequenced strains was
350 365x as compared to 59x for the twelve strains sequenced in our hands, while the average
351 PacBio read N50 for the previously sequenced strains was 5.73 kb as compared to
352 11.65kb for the strains sequenced by our lab.
353
354 Libraries for Illumina sequencing were made for all 18 founder strains. The same genomic
355 DNA that had been used to prep the SMRTbell libraries was used to make Illumina
356 libraries. Genomic DNA from the six remaining strains was prepared using the Qiagen G-
357 tip kit as above. All genomic DNA was sheared to ~300-400bp using the Covaris S220
358 Focused Acoustic Shearer with the following settings: peak incident power (w) of 140,
359 Duty Factor of 10%, Cycles per Burst of 200, Treatment time of 65s, temperature of 4°C,
360 and water 12. Illumina compatible libraries were prepared using the NEBNext Ultra II DNA
361 Library Prep kit along with the NEBNext Multiplex Oligos for Illumina (Index Primer Set 1)
362 as per the manufacturer's recommendations. Adaptor-ligated DNA was size-selected and
363 PCR-enriched for five cycles, followed by clean-up of the PCR reaction using AMPure XP

Beads as per the NEBNext Ultra II DNA Library Prep protocol. Sequencing was carried out using the Illumina HiSeq4000 with PE100 or PE150 reads (see Note S3). The average per-site coverage of the 18 founder strains was 290x with the lowest coverage being 186x (founder B11) and the highest coverage at 374x (founder AB4).

Genome assembly

We assembled the PacBio reads using canu v1.7 (commit r8700; options: corMhapSensitivity=high, corOutCoverage=500, minReadLength=500, corMinCoverage=0, correctedErrorRate=0.105) (Koren *et al.* 2017). We generated hybrid assemblies using the PacBio and Illumina reads for the twelve strains for which we generated the PacBio reads. The PacBio reads from the six strains from (Yue *et al.* 2017) were too short to assemble with DBG2OLC, the hybrid assembler we use (Ye *et al.* 2016). The DBG2OLC hybrid assemblies were used to fill gaps in the corresponding canu assemblies using quickmerge, following the two steps merging approach (Chakraborty *et al.* 2016; Solares *et al.* 2018). The PacBio reads from Yue et al. were sequenced using an older chemistry of Pacific Biosciences (P4-C2) than our PacBio reads (P6-C4), so they required a different algorithm for optimal polishing than the assemblies created with the P6-C4 reads. Hence, we polished the P4-C2 based assemblies twice using Quiver and the P6-C4 based assemblies twice using Arrow (smrtanalysis v5.2.1). Finally, we polished all assemblies twice with the paired end Illumina reads using Pilon (Walker *et al.* 2014).

BUSCO assessment

386 We estimated the number of fungi BUSCOs (n=290) in each polished assembly using
387 BUSCO v3.0.2 (Waterhouse *et al.* 2018) (Table 2). For the augustus gene prediction step
388 in BUSCO we used 'saccharomyces_cerevisiae_S288C' as the species option.
389
390 *QV estimate*
391 To estimate assembly error rate, paired end Illumina reads used in assembly polishing
392 were mapped to the final assembly using bowtie2 (Langmead and Salzberg 2012). SNPs
393 and small indels were identified using freebayes v0.9.21 (-C 10 -0 -O -q 20 -z 0.10 -E 0 -
394 X -u -p 1 -F 0.75) (Garrison and Marth 2012a). To estimate the error rate, total bases due
395 to SNPs and small indels (e) and the total number of assembly bases (b) with read
396 coverage ≥3 were counted and qv was calculated as –10 X log(e/b) (Koren *et al.* 2017)
397 (Table 2).
398
399 *Santa Cruz Browser Tracks*
400 Assembled genomes were aligned to one another and the *SacCer3* reference genome
401 using *ProgressiveCactus* (https://github.com/ComparativeGenomicsToolkit/cactus)
402 (Paten *et al.* 2011a, 2011b). Santa Cruz Browser Track Hubs were created using the
403 *hal2assemblyhub* script that is part of the *ProgressiveCactus* software
404 (https://github.com/ComparativeGenomicsToolkit/Comparative-Annotation-Toolkit). The
405 resulting SNAKE tracks are viewable at http://bit.ly/2ZrreUd. SNPs were identified
406 between the founder strains using a generic GATK pipeline, with SNPs functionally
407 annotated using SNPeff (Cingolani *et al.* 2012). Scripts to align the genomes and call
408 SNPs in the founders are available here: https://github.com/tdlong/yeast_resource.

Analysis of structural variants

We aligned each founder genome assembly to the s288c reference genome (GCA_000146055.2) using MUMmer v4.0 (Marçais *et al.* 2018) (nucmer --maxmatch --prefix founder ref.fasta founder.fasta). To annotate the SVs, the delta alignment file for each strain was then processed with SVMU (commit e9c0ea1) (Chakraborty *et al.* 2019).

Whole genome sequencing of the two base populations

The two base populations were deeply sequenced using Illumina technology. In total, 4mL of the 18F12v1 frozen stock was thawed at RT, pelleted at 3000 RPM for 5m, and resuspended in 20mL of YPDamp. This was followed by incubation at 30°C for 3.5h at 275RPM. Genomic DNA was extracted using the Qiagen DNeasy kit. The genomic DNA was sheared using the Covaris S220 as above and Illumina compatible libraries were prepared using the NEBNext Ultra II DNA Library Prep kit as above. The NEBNext and libraries were pooled and sequenced on the HiSeq4000 using PE100 reads. The NEBNext libraries were sequenced at a mean per-site coverage of 3270x.

For 18F12v2, similarly to 18F12v1, 4mL of frozen stock was thawed at RT, pelleted at 3000RPM for 5m, and resuspended in 20mL of YPDamp, followed by incubation at 30°C for 3.5h at 275RPM. Genomic DNA was extracted using the Qiagen G-tip kit. Nextera libraries were prepped for 18F12v2 by following the standard Nextera protocol with slight modifications. Tagmentation reactions were carried out in 2.5uL reactions for 10m at 55°C. Reactions were stopped by adding SDS to a final concentration of 0.02% followed

by incubation at 55°C for 7m. Samples were immediately transferred to ice. Limited cycle PCR was carried out to add two unique barcodes to each library to enable dual index sequencing. This avoids the problem of barcode switching when *N* i7 and *M* i5 barcodes are used to create *MN* combinations. The KAPA HiFi Ready Mix (2X) was used in conjunction with the KAPA forward and reverse primers to amplify tagmented libraries in 25uL total volume. Thermocycling parameters consisted of 3m at 72°C, 5m at 98°C, followed by 15 cycles of 10s at 98°C, 30s at 63°C, and 30s at 72°C, with a hold of 72°C for 5m at the end. PCR reactions were cleaned up using AMPure XP Beads (Beckman Coulter, Inc.) and libraries quantified by Qubit. Sequencing was performed on the HiSeq4000 using PE150 reads. 18F12v2 libraries received 2226x coverage.

Whole genome sequencing of the first two meiotic generations of the second base population

For 18F1v2 and 18F2v2, ~1mL of frozen stock was thawed at RT, spun down at 7500 RPM for 5m in microcentrifuge tubes, resuspended in 1mL of YPDamp, transferred to a 250mL flask with 19mL of YPDamp and incubated at 30°C for 3.5h at 275RPM. Genomic DNA from both samples was extracted using the Qiagen G-tip kit. Nextera libraries were prepped by following the Nextera flex protocol using 1/5th reactions with slight modifications. Limited cycle PCR was carried out using the KAPA HiFi Ready Mix (2X) as detailed above to add barcoded Illumina-compatible adapters in 12.5uL reactions. Thermocycling parameters consisted of 3m at 72°C, 3m at 98°C, followed by 12 cycles of 45s at 98°C, 30s at 62°C, and 2m at 72°C, with a hold of 72°C for 1m at the end. Proteinase K was added to each reaction (50ug/mL final concentration) to digest the

455 polymerase. Samples were incubated for 30m at 37°C and 10m at 68°C. Reactions were
456 cleaned up using the SPB beads provided with the Nextera flex kit. Sequencing was
457 performed as above using PE100 reads. 18F1v2 received 98x coverage while 18F2v2
458 received 73x coverage.
459
460 *Whole genome resequencing of recombinant haploid clones*
461 Ten haploid recombinant clones (5 of each mating type) were isolated from each of the
462 two base populations. 18F12v1-derived haploids were generated by sporulating an O/N
463 culture of the 18F12v1 population in 2mL of PA7 in a 10mL culture tube at 30°C for 3d.
464 Spore isolation and dispersal were carried out as detailed above for the creation of
465 18F12v2 with 15m of bead milling to disperse spores. Spores were plated at low density
466 onto YPD plates and incubated for 2d at 30°C. One of the YPD plates was then replica
467 plated onto four different plates: YPD with hyg, YPD with cloNAT, YPD with mate-type
468 tester 1, and YPD with mate-type tester 2. Five haploids of each mating type were
469 inoculated into YPD O/N. Genomic DNA was extracted using the Qiagen DNeasy kit and
470 Nextera libraries prepared as above. Libraries were sequenced on a HiSeq4000 using
471 PE100 reads to a mean per-site coverage of ~32x.
472
473 18F12v2-derived haploids were generated by sporulating an O/N culture of the 18F12v2
474 population in 4mL of PA7 in a 24 deep-well plate at 30°C at 275RPM for 3d. Spore
475 isolation and dispersal were carried out as detailed above for the creation of 18F12v2
476 with 20m of bead milling to disperse spores. Spores were plated at low density onto YPD
477 plates and incubated at 30°C for 3d. 96 single colonies were then transferred into a 96

478 deep-well plate with YPDamp using sterile toothpicks. After O/N incubation at 30°C,
479 200uL of culture from each well was transferred to a 96 shallow plate and pinned YPD
480 plates with either cloNAT, hyg, mate-type tester 1, or mate-type tester 2 using a 48-well
481 replicator tool. The source plate was covered with an adhesive membrane and stored at
482 4°C. The mate typing plates were incubated at 30°C for 2d, after which five haploids of
483 each mating type were transferred from the original source plate to 1.5mL eppendorfs
484 and genomic DNA was extracted using the Qiagen DNeasy kit. Nextera libraries were
485 prepared as above. Libraries were sequenced on a HiSeq4000 using PE150 reads to a
486 mean per-site coverage of ~60x.
487
488
489 *Haplotype calling in Illumina resequenced MPPs and recombinant haploid clones*
490 De-multiplexed fastq files were used in analyses. Detailed scripts/software versions to
491 reproduce our analysis are located at https://github.com/tdlong/yeast_resource.git.
492 Briefly, reads were aligned to the *sacCer* reference genome using *bwa-mem* and default
493 parameters (Li and Durbin 2009; Li 2013). We maintain two SNP lists, a set of known
494 SNPs in the strains obtained from a GATK pipeline that only considers the isogenic
495 founders, and a subset of those SNPs that are well-behaved (i.e., frequency of the REF
496 allele close to zero or one in all founder lines, pass GATK qualify filters, etc.). The list of
497 well-behaved SNPs that are polymorphic in the founders can be used to speed-up
498 subsequent steps, where we sometimes examine hundreds of samples, since only
499 variants polymorphic among the founders need be considered when working with
500 samples from a synthetic population (except when calling newly arising mutations).

samtools mpileup (Li *et al.* 2009; Li 2011) and *bcftools* (Narasimhan *et al.* 2016) are used to query well-behaved known SNPs. We have no interest in calling genotypes, but instead simply output the frequency of the REF allele in each sample at each location (output=SNPtable). In a separate analysis *freebayes* (Garrison and Marth 2012b), *vcfallelicprimitives* (https://github.com/vcflib/vcflib), and *vt normalize* (Tan *et al.* 2015) are used to call all SNPs, and the SNPs not in our list of known SNPs considered candidate new mutations.

We have developed custom software to infer the frequency of each founder haplotype at each location in the genome in pooled samples using the SNPtable as input and the *haplotyper.limSolve.code.R* script in the github archive. This same algorithm can also be used without modification to infer genotypes in recombinant haploid clones. Briefly, we slide through the genome in 1kb steps considering a 60kb window for each step. For all SNPs in the window we calculate a Gaussian weight such that the 50 SNPs closest to the window center account for 50% of the sum of the weights. We then consider F founders and use the *lsei* function of the *limSolve* package (*limSolve: Solving Linear Inverse Models*, R package 1.5.1) (Meersche *et al.* 2009) in *R* to identify a set of F mixing proportions (each greater than zero and summing to one) that minimize the sum of the weighted squared differences between founder haplotypes and the observed frequency of each SNP in a pooled sample. That is, for a N SNP window we call *lsei* with the following parameters: A=N*F matrix of founder genotypes, B=N*1 vector of SNP frequencies in a pooled sample, E=F*1 vector of 1's, F=1, G=F*F identity matrix, H= F*1 vector of 0's, and Wa=N*1 vector of weights. Finally, for windows where the i^{th} and j^{th}

524 founders have near indistinguishable haplotypes, implying the sum of the two mixing
525 proportions are correct, but not individual estimates, we estimate the haplotype frequency
526 as half the sum of the two mixing proportions. This method of accounting for
527 indistinguishable haplotypes is regional and is generalized to more than two near identical
528 founders and multiple such sets.
529
530 *Validation of the haplotype caller*
531 In order to validate our haplotype-calling algorithm, we identified 70,478 SNPs private
532 to a single founder strain (excluding those present in founders merged due to high
533 sequence similarity). The haplotype caller was run on 18F12v2 using the full coverage
534 data (i.e., 2230X) or down-sampled 18F12v2 to simulate a more typical poolseq re-
535 sequencing depth (typical applications using the MPPs are likely to sequence hundreds
536 of experimental units to ~20-60X). For each private SNP, the frequency of the SNP in the
537 full coverage data was estimated and the founder harbouring that SNP identified. Since
538 the sequence depth of the non-downsampled population is 2230X, the frequency of each
539 private SNP is measured very accurately. We then infer the frequency of the founder
540 haplotype harbouring the private SNP at the position closest to the private SNP, in both
541 the full coverage and each downsampled population. The error rate associated with the
542 haplotype caller is the absolute difference between frequency of each private SNP and
543 the founder haplotype harbouring it.
544
545 In our examination of the relationship between haplotype and SNP frequency estimates
546 (Figure 4) we identified and removed 91 outlier SNPs among the 71,301 private SNPs.

These SNPs were identified as private SNPs whose frequency was more than 5% different than the frequency of the haplotype harbouring it in the full dataset, while exhibiting flanking private SNPs in the same founder whose frequency agree with the founder frequency. We believe these outlier SNPs are cases where that particular SNP in a pooled sample cannot be aligned to the reference genome very accurately. It is noteworthy that it is more difficult to identify poorly performing SNPs that are not private to a single founder, and such SNPs likely hurt haplotype inference methods.

Delineating haplotype blocks in recombinant haploid clones

The haplotype caller is primarily used to estimate the frequency of founder haplotypes at different positions in the genome in a DNA pool from a segregating population, but it can also be run on DNA obtained from a haploid or diploid clone. In a haploid clone the haplotype caller should return a haplotype frequency of close to 100% for one of the founder haplotypes for much of the genome, with sharp transitions between founder states near recombination breakpoints. In depicting the haplotypic structure of haploid clones we classify genomic regions at which the inferred haplotype frequency of a single founder (or multiple indistinguishable founders) is less than 95% as having an 'unknown' haplotype (these unknown intervals typically being associated with state transitions). We also observe intervals in which several founders are indistinguishable from one another (due to insufficient SNP divergence between the founders in these window). We could sometimes resolve these intervals to a single founding haplotype when flanking haplotypes were unambiguously called as derived from the same single founder. Custom R scripts were used for these analyses as well as to calculate the length of haplotype

570 blocks in haploid clones. Haplotype block sizes were inferred by finding the positional
571 difference between the beginning and end of runs of the same haplotype.
572
573 *Data and reagent availability*
574 Strains and plasmids are available upon request. All genome sequencing data and
575 assemblies have been deposited into public repositories. Sequence data generated for
576 the two base populations (18F12v1, 18F12v2, 18F1v2, and 18F2v2) as well as the
577 recombinant haploid clones are available in the Short Reads Archive under the bioproject
578 PRJNA551443 in accessions SRX6465384 to SRX6465405 and SRX6983898 to
579 SRX6983899. All PacBio and Illumina data generated for the 18 founding strains is also
580 available in the Short Reads Archive under the bioproject PRJNA552112 in accessions
581 SRX6380915 to SRX6380944. Detailed scripts/software versions to reproduce our
582 analysis are located at https://github.com/tdlong/yeast_resource.git.
583
584 **Results and Discussion**
585 *Recovery of hyg^r and insertion of dominant selectable markers for high-throughput diploid*
586 *selection*
587 We further engineering a subset of the yeast SGRP resource strains (Cubillos *et al.* 2009)
588 to serve as founders for an 18-way synthetic population. We first recovered the *hyg^r*
589 marker used to delete the *HO* gene in the haploid SGRP strains. Previous work
590 (McDonald *et al.* 2016) replaced *YGR043C*, a pseudogene that is physically close to the
591 mating type locus, with dominant selectable markers in order to facilitate high-throughput
592 selection of diploids after mating. We echoed that approach here by replacing YGR043C

593 with *NatMX4* in 15 *Mat a* (or "A") founders and with *HphMX4* in 15 *Mat α* (or "B" founders).
594 The presence of these cassettes confers resistance to the antibiotics nourseothricin and
595 hygromycin B, respectively, enabling the selection of doubly resistant diploids. All newly
596 engineered strains are given in Table 1.
597
598 *de novo assembly of high-quality reference genomes for the 18 founding strains*
599 We generated *de novo* genome assemblies for the founders used to create our MPPs
600 using a hybrid sequencing strategy detailed in (Chakraborty *et al.* 2016) that involves
601 using a combination of long-read (PacBio) and short-read (Illumina paired-end)
602 sequencing technology. The *de novo* assemblies allow us to reliably identify structural
603 variants while the overall assembly has a low per base pair error rate. We assembled
604 58.9X PacBio reads on average (33-90X) for 12 of the founder strains, and re-assembled
605 the other six strains using publicly available shorter length 364.9X PacBio reads on
606 average. Despite the different number and chemistry of PacBio reads used in assembling
607 the genomes, all of our assemblies are highly accurate (average qv = 52.5) and show
608 comparable contiguity. For example, the average contig N50 of our assemblies is ~800Kb
609 (N50 = 50% of the assembly is contained within sequences of this length or longer),
610 indicating that the majority of the chromosomes are represented as single contigs (Table
611 2). Examination of 290 conserved fungal single copy orthologs (Benchmarking Single
612 Copy Orthologs or BUSCO) show that completeness (~99%) of all our assembled
613 genomes is comparable to the reference S288C assembly (99%).
614

We aligned the assemblies to one another and represent them as Santa Cruz genome browser tracks (http://bit.ly/2ZrreUd). These tracks have utility when looking for candidate causative variants in small regions of genetic interest. The large amount of genetic diversity sampled by the founders can be illustrated by zooming in on regions such as that shown in Figure 2, which highlights the numerous alleles segregating at a gene implicated in many genetic mapping studies in budding yeast, the highly pleiotropic *MKT1*. *MKT1* influences several cellular processes including the DNA damage response, mitochondrial genome stability, drug resistance, and post-transcriptional regulation of *HO* (Dimitrov *et al.* 2009; Ehrenreich *et al.* 2010; Tkach *et al.* 2012; Kowalec *et al.* 2015a). Studies have found that different alleles of *MKT1* can differentially affect several phenotypes, including mitochondrial genome stability and drug resistance. Variation at this gene amongst our founders includes ten nonsynonymous SNPs and thirty-four synonymous SNPs. Of the ten nonsynonymous SNPs, six are predicted to change the secondary structure of the protein. Taking into account only nonsynonymous SNPs, there are seven different alleles segregating amongst the founders (all segregating in our 18F12v2 MPP).

The genome browser tracks are also useful for visualizing structural variants such as those shown in Figure 3, which highlights a large (>1kb) deletion in the vacuolar ATPase *VMA1* (Figure 3A) present in half of the founders. Previous work has shown that the deleted region encodes a self-splicing intein, PI-SceI, a site-specific homing endonuclease that catalyzes its' own integration into inteinless alleles of *VMA1* during meiosis (Gimble and Thorner 1992). This selfish genetic element has been shown to

638 persist in populations solely through horizontal gene transfer and is present in many
639 species of yeast. Perturbation of *VMA1* itself has been shown to influence both replicative
640 and chronological lifespan, resistance to metals, as well as oxidative stress tolerance
641 (Kane 2007; Ruckenstuhl *et al.* 2014).
642
643 In addition to large deletions, copy number variants (CNVs) can also be found, such as
644 that shown in Figure 3B, in which the cytoplasmic aldehyde dehydrogenase, *ALD2,* is
645 duplicated in founder A5. Conversely, this gene has been deleted in founders B5 and B8.
646 *ALD2* has been shown to be involved in the osmotic stress response as well as the
647 response to glucose exhaustion (Navarro-Aviño *et al.* 1999). A more structurally complex
648 region was identified on Chromosome VII (Figure 3C) at which multiple different deletions
649 (ranging from ~50bp to >300bp) were found to occur at *MSB2*, an osmosensor involved
650 in the establishment of cell polarity (O'Rourke and Herskowitz 2002; Cullen *et al.* 2004).
651 Null alleles of *MSB2* have been shown to have decreased chemical resistance.
652
653 One of the most structurally complex regions we identify contains ~2kb of repetitive
654 sequence and is present on chromosome IV (Figure 3D and E as well FigureS1) at which
655 multiple different deletions (ranging from ~80bp to >500bp) as well as duplications occur
656 in multiple founders within the *PRM7* and *BSC1* genes. Due to the highly complex nature
657 of the variation present, this region is represented as a series of dot plots, with two
658 founders highlighted in the main text (Figure 3D and E). Dot plots of this region in all
659 founder strains are shown in FigureS1. A previous study demonstrated that although two
660 distinct genes (*PRM7* and *BSC1*) are present in S288C, a combination of small deletions

and point mutations in another yeast strain (W303) have caused the STOP codon to be absent from *BSC1*, leading to the read-through transcription of a new gene that encompasses sequence from both *PRM7* and *BSC1* as well as the intergenic region between them (Kowalec *et al.* 2015b). This gene, *IMI1*, was shown to affect mtDNA stability as well as intracellular levels of reduced glutathione (GSH).

The above regions highlight the utility of our *de novo* genome assembly approach, as deletions and CNVs of this scale would be difficult to detect via the usual method of aligning short reads to a reference genome. But if an investigator mapped a QTL to one of these genes they would certainly want to know about the existence of the segregating structural variation.

Despite the large amount of natural variation present amongst the founders in general, some of the founders were found to be genetically very similar to one another (AB3/B6) Figure S2 and shown in Table S4), having less than 200 pairwise SNP differences. This lack of divergence makes this set of founders difficult to distinguish from one another for much of the genome and as a result we collapse them for subsequent analyses (despite that fact that a subset of these 200 differences could be functional). Three additional founders (A11/A12/B11) were also found to be highly genetically similar to one another, with, on average, less than 2,000 pairwise SNP differences. These differences are concentrated in a small number of regions, making these three founders distinguishable for these regions (but indistinguishable for much of the remainder of the genome). We keep these strains separate for downstream analyses.

Creation of two 18-way highly outcrossed populations

MPPs created using multiple rounds of recombination can significantly increase the resolution of genetic mapping studies by virtue of haplotypes sampled from these population having a greater number of genetic breakpoints. Furthermore, multiple founders results in high levels of standing variation present in the MPP. These two features result in populations that more realistically mimic natural outbred diploid populations, and samples more functional alleles and haplotypes from the species as a whole than a two-way cross. With these goals in mind, we constructed a large, genetically heterogenous population by crossing 18 different founder strains (each strain being derived from the SGRP (Cubillos *et al.* 2009)). The 18 founder strains were chosen to represent a broad swathe of the natural diversity of the species and belong to diverse phylogenies, including: Wine/European, West African, North American, Sake, and Malaysian (see Table 1). It is also noteworthy that founder strains A1-4 and B1-4 are the same four strains using in (Cubillos *et al.* 2013), and were introduced into the population as both *Mat a* and *Mat α* mating types. We created two versions of our 18-way MPP. In both cases a full diallele cross was used to create all 121 unique diploid genotypes from 11 *Mat a* and 11 *Mat α* strains (see Figure 1A and B). All 121 diploid genotypes were combined and the resulting population was taken through 12 rounds of sporulation followed by random mating to break up linkage disequilibrium. Previous work has shown that 12 rounds of random recombination breaks up haplotype blocks to the point where additional outcrossing does not significantly decrease LD (Parts *et al.* 2011). For brevity, the two different outcrossed populations will be referred to as 18F12v1 and 18F12v2,

707 respectively, throughout the rest of this manuscript. The version 1 MPP differed primarily
708 from version 2 in that the 121 diploid genotypes obtained from the diallele were directly
709 combined and sporulated *en masse* (version 1; Figure 1A) to create the MPP, as opposed
710 to being individually carried through sporulation and spore disruption before being
711 combined (version 2; Figure 1B). Furthermore, due to a technical artefact during the 12
712 rounds of outcrossing, 18F12v1 is cross-contaminated with the 4-way F12 population
713 from (Cubillos *et al.* 2013) which contains a functional URA3 gene. As a result, 18F12v1
714 MPP is of limited utility for experiments that require uracil auxotrophy, and 18F12v2 is the
715 current primary focus of work in our lab.
716
717
718 *Development of an algorithm for accurately inferring haplotype frequencies*
719 In QTL mapping experiments using MPPs it is often advantageous to map QTLs back to
720 founder haplotypes. In experiments derived from a two way cross between isogenic
721 founders genotyping SNPs accomplishes this, but with multiple founders parental
722 haplotypes have to be inferred in recombinant offspring (Mott *et al.* 2000). In a similar
723 manner when MPPs are used as a base population and genetic changes detected
724 following an experimental treatment it is often of value to examine changes in haplotype
725 frequency (as done in (Burke *et al.* 2014) and reviewed in (Barghi and Schlötterer 2019)).
726 We developed a sliding window haplotype caller that can be used in the situation when
727 the founder haplotypes are known and apply it to both single haploid clones and pools
728 consisting of millions of diploid individuals. This haplotype caller differs from other widely
729 used callers (Long *et al.* 2011; Kessner *et al.* 2013) in that it acknowledges that in some

730 windows pairs of founders are poorly resolved or indistinguishable and relies solely on
731 read counts at known SNP positions in both founders and recombinant populations.
732
733 To benchmark the haplotype-calling algorithm, we compared the frequency of SNPs
734 private to a single founder to the haplotype frequency of the same founder for the interval
735 closest to the SNP location in the 18F12v2 base population. Since this base population
736 is sequenced to 2226X we initially wished to look at the error in the haplotype estimate at
737 full coverage where the sampling variation on the SNP frequency estimate is quite low
738 (proportional to 1/sqrt(2226) or <2%). For the high coverage base population regions
739 showing large difference between SNP and haplotype frequency estimates likely
740 represent instances where the haplotype caller breaks down, since we attempted to
741 remove SNPs whose frequencies are poorly estimated. Figure S3, depicting the absolute
742 difference in SNP versus haplotype frequency differences, shows that haplotype and SNP
743 frequencies generally agree with one another with average and median error rates of
744 0.4% and 0.2%, respectively (below the sampling error of SNP frequency).
745
746 Of course, typical experiments employing these base populations will sample the
747 population following some treatment, and comparing haplotype frequencies in control
748 versus treated samples. Although the 18F12v2 base population is sequenced to 2226X,
749 it would be cost-effective if we could infer haplotype frequencies from pooled samples
750 sequenced to much lower coverage. To determine the accuracy of our haplotype
751 estimates as a function of sequencing coverage the 18F12v2 was down-sampled 50-fold
752 and 100-fold, which corresponds to poolseq datasets of ~40X and ~20X respectively. We

753 then estimated relative haplotype frequency error rates as a function of sequence
754 coverage (Figure S3b) and absolute error rates as a function of coverage and genomic
755 location (Figure S4). It is apparent that the error rate is an increasing function of
756 decreasing coverage, but for much of the genome the absolute error in haplotype
757 frequency estimate is actually lower than the binomial sampling errors associated with
758 directly estimating SNP frequencies at the same coverage (*i.e.,* at 20-40X coverage
759 binomial sampling errors on frequency are >10%). It is also apparent that the average
760 error rate is likely driven by a few regions where the haplotype caller struggles; these are
761 presumably regions with poor divergence between founders in the window examined.
762 Overall the mean (median) error rates on haplotype frequency estimates are low, 1.3%
763 (0.8%) at 20X and 1% (0.6%) at 40X, respectively.
764
765
766 **Table 3.** Mean haplotype frequencies in 18F12v1 and 18F12v2

Founder	18F12v1_frequency	18F12v2_frequency
AB1	4.4%	1.2%
AB2	3.8%	0.5%
AB3	10.6%	41.4%
AB4	5.8%	3.3%
A5	1.2%	14.0%
A6	0.8%	14.3%
A7	2.4%	0.4%
A8	1.2%	0.7%
A9	0.1%	0.5%
A11	9.9%	1.2%
A12	18.1%	1.7%
B5	27.1%	11.3%
B7	1.1%	1.0%
B8	0.5%	5.7%
B9	0.9%	0.8%

B11	9.8%	1.3%
B12	2.4%	0.6%

767

768 *Characterization of 18F12v1 and 18F12v2 base populations*

769 18F12v1 and 18F12v2 were subjected to high coverage whole-genome sequencing to
770 both characterize their population structure and to establish a baseline for future mapping
771 studies. Figures 5 and 6 show the inferred sliding window haplotype frequencies for
772 18F12v1 and 18F12v2, respectively, while Table 3 shows the mean per founder
773 haplotype frequencies genome-wide. One trend that is evident is that in both the 18F12v1
774 and 18F12v2 MPPs a small number of founders are over-represented. In order to identify
775 the origin of this bias, at least for 18F12v2, the first two meiotic generations of 18F12v2
776 were sequenced (Figures S5 and S6; Table S5). Despite having an initially more balanced
777 population after the first round of random mating, a few strains quickly became
778 disproportionately over-represented. One possible explanation for this is that a few
779 founding haplotypes were selected for early in the twelve rounds of intercrossing. Figure
780 S7 provides suggestive evidence that this may have been the case, as the frequency of
781 hapotypes derived from founder A5 increase genome-wide after the second round of
782 meiosis. The latter half of chromosome XIII (from founder A5) emphasizes this point as it
783 was very highly selected for initially. Another potential source of bias was the pooling
784 strategy, which was done using optical density as a proxy for cell numbers. This may have
785 resulted in an uneven distribution of founders in the initial pool. Nonetheless, after 12
786 rounds of random mating, deep sequencing of 18F12v2 revealed that haplotypes from all
787 founding strains were present in the population at a detectable frequency (Table 3).
788 Specifically, haplotypes from ten or more founders were detected as segregating in over

789 99% of the genome in 18F12v2 and close to 98% of the genome in 18F12v1.
790 Furthermore, 18F12v2 was verified to be auxotrophic for uracil, facilitating future
791 manipulations for downstream analyses.
792
793 *Characterizing the recombination landscape of 18F12v1- and 18F12v2-derived*
794 *segregants*
795 In order to further characterize 18F12v1 and 18F12v2, ten haploid segregants were
796 generated from each diploid population and subjected to whole-genome sequencing. The
797 complex structure of these populations is highlighted in Figure 7. The mean (median) size
798 of haplotype blocks in 18F12v1-generated segregants was 103kb (66kb) while the mean
799 (median) size of haplotype blocks in 18F12v2-generated segregants was 106kb (66kb)
800 (Figure S8). The mean number of discrete haplotype blocks in 18F12v1-generated
801 segregants was 106 as compared to 104 in 18F12v2-generated segregants. A previous
802 study (Cubillos *et al.* 2013) found that twelve rounds of meiosis in a yeast 4-way cross
803 resulted in a median block size of 23kb with 374 discrete haplotype blocks. Some of the
804 failure to obtain the smaller block sizes and more numerous discrete blocks of this
805 previous study may be due to undetectable recombination events occurring within
806 haplotypes over-represented in our populations. Another possibility is that, due to the
807 large number of founding haplotypes, recombination events were missed in regions at
808 which multiple founding strains are highly genetically similar. It is also possible that some
809 of the founding strains used in this study have relatively low natural recombination rates.
810

To highlight the diversity present in the two outbred populations, a close-up view of inferred haplotypes in segregants derived from each population at chromosome X is shown in Figure S9. Regions in which the founding haplotype is unknown tended to occur at the transitions between haplotypes (see Note S4) and are a mean (median) length of 7.8kb (6kb) in 18F12v1-derived segregants and 7.5kb (6kb) in 18F12v2-derived segregants. Also noticeable is, at least for this chromosome, the larger amount of variation segregating in 18F12v2 (Figure S9B).

Conclusion

The paradigm of utilizing pairwise crosses to dissect the genetic basis of complex traits has enjoyed much success in diverse model organisms. However, such studies typically underestimate the standing variation present in natural populations and often lack the resolution to pin-point causal variants to a small number of genes. Conversely, association studies are typically underpowered to detect rare alleles, poorly tagged variants, and regions with multiple causal sites in weak LD with one another. MPPs have been proposed to bridge the gap between the above two approaches. Although MPPs have been created in several model systems, only a single MPP has thus far been described in budding yeast. By generating two large, highly outcrossed and genetically heterogeneous populations of *S. cerevisiae* derived from eighteen different founder strains, we have created a powerful resource that can be used in a variety of experimental settings. For instance, these populations can be used in large-scale X-QTL mapping experiments (Ehrenreich *et al.* 2010) to comprehensively dissect the genetic architecture of complex traits as well as large-scale evolve and re-sequence experiments (Lang *et al.*

2011; Parts *et al.* 2011; Burke *et al.* 2014) to determine the mechanisms and course of adaptation to diverse stimuli. Large number of recombinant haploid clones generated from these populations can be used in complementary large-scale I-QTL studies (Bloom *et al.* 2013; Wilkening *et al.* 2014). Due to the high levels of standing variation present, these populations should also prove to be a powerful resource in evolutionary engineering applications, as they are presumably capable of being evolved to carry out a plethora of useful tasks.

The haplotype calling software generated in this study represents a useful resource for the MPP community in general, as it enables highly accurate haplotype calling in poolseq data at reduced coverage. The ability of the algorithm to deal with windows where all founder haplotypes cannot be resolved will have utility in a subset of systems, including our yeast populations. Candidate causal regions can be identified by comparing haplotype frequencies at discrete intervals across the genome in control versus treatment populations. Candidate regions can then be examined in the UCSC genome browser, where genome-wide alignments of all founder strains have been posted. Structural variants can be easily visualized in the browser as can nonsynonymous SNPs, thus pointing investigators to potentially causal genes.

In conclusion, the populations generated in this study represent a novel resource that brings together the power of QTL mapping, the resolution of association studies, and a large amount of natural variation to a model system capable of teasing apart and directly testing the molecular underpinnings of complex traits.

Acknowledgments

We thank the UC Irvine Genomics High Throughput Facility for the quick turn-around and efficient processing of libraries for sequencing and for help with figuring out the parameters for the Covaris S220 Focused Acoustic Shearer. We would also like to acknowledge our funding source: NIH grant FG18445 to ADL.

References

Aylor, D. L., W. Valdar, W. Foulds-Mathes, R. J. Buus, R. A. Verdugo *et al.*, 2011 Genetic analysis of complex traits in the emerging Collaborative Cross. Genome Res. 21: 1213–22.

Barghi, N., and C. Schlötterer, 2019 Shifting the paradigm in Evolve and Resequence studies: From analysis of single nucleotide polymorphisms to selected haplotype blocks. Mol. Ecol. 28: 521–524.

Berg, J. J., A. Harpak, N. Sinnott-Armstrong, A. M. Joergensen, H. Mostafavi *et al.*, 2019 Reduced signal for polygenic adaptation of height in UK Biobank. Elife 8:.

Bloom, J. S., J. Boocock, S. Treusch, M. J. Sadhu, L. Day *et al.*, 2019 Rare variants contribute disproportionately to quantitative trait variation in yeast. bioRxiv 607291.

Bloom, J. S., I. M. Ehrenreich, W. Loo, T.-L. V. Lite, and L. Kruglyak, 2013 Finding the sources of missing heritability in a yeast cross. Nature 494: 234.

Bloom, J. S., I. Kotenko, M. J. Sadhu, S. Treusch, F. W. Albert *et al.*, 2015 Genetic interactions contribute less than additive effects to quantitative trait variation in yeast. Nat Commun 6: 8712.

Burke, M. K., G. Liti, and A. D. Long, 2014 Standing genetic variation drives repeatable

881 experimental evolution in outcrossing populations of Saccharomyces cerevisiae.
882 Mol. Biol. Evol. 31: 3228–39.
883 Chakraborty, M., J. G. Baldwin-Brown, A. D. Long, and J. J. Emerson, 2016 Contiguous
884 and accurate *de novo* assembly of metazoan genomes with modest long read
885 coverage. Nucleic Acids Res. 44: gkw654.
886 Chakraborty, M., J. J. Emerson, S. J. Macdonald, and A. D. Long, 2019 Structural
887 variants exhibit widespread allelic heterogeneity and shape variation in complex
888 traits. Nat. Commun. 10:.
889 Chen, G.-B., S. H. Lee, M. R. Robinson, M. Trzaskowski, Z.-X. Zhu *et al.*, 2017 Across-
890 cohort QC analyses of GWAS summary statistics from complex traits. Eur. J. Hum.
891 Genet. 25: 137–146.
892 Cingolani, P., A. Platts, L. L. Wang, M. Coon, T. Nguyen *et al.*, 2012 A program for
893 annotating and predicting the effects of single nucleotide polymorphisms, SnpEff:
894 SNPs in the genome of Drosophila melanogaster strain w1118; iso-2; iso-3. Fly
895 (Austin). 6: 80–92.
896 Cubillos, F. A., C. Brice, J. Molinet, S. Tisné, V. Abarca *et al.*, 2017 Identification of
897 Nitrogen Consumption Genetic Variants in Yeast Through QTL Mapping and Bulk
898 Segregant RNA-Seq Analyses. G3 (Bethesda). 7: 1693–1705.
899 Cubillos, F. A., E. J. Louis, and G. Liti, 2009 Generation of a large set of genetically
900 tractable haploid and diploid *Saccharomyces* â€ƒstrains. FEMS Yeast Res. 9:
901 1217–1225.
902 Cubillos, F. A., L. Parts, F. Salinas, A. Bergström, E. Scovacricchi *et al.*, 2013 High-
903 resolution mapping of complex traits with a four-parent advanced intercross yeast

904 population. Genetics 195: 1141–55.

905 Cullen, P. J., W. Sabbagh, E. Graham, M. M. Irick, E. K. Van Olden *et al.*, 2004 A

906 signaling mucin at the head of the Cdc42- and MAPK-dependent filamentous

907 growth pathway in yeast. Genes Dev. 18: 1695–1708.

908 Dimitrov, L. N., R. B. Brem, L. Kruglyak, and D. E. Gottschling, 2009 Polymorphisms in

909 multiple genes contribute to the spontaneous mitochondrial genome instability of

910 Saccharomyces cerevisiae S288C strains. Genetics 183: 365–383.

911 Ehrenreich, I. M., N. Torabi, Y. Jia, J. Kent, S. Martis *et al.*, 2010 Dissection of

912 genetically complex traits with extremely large pools of yeast segregants. Nature

913 464: 1039–42.

914 Flint, J., and R. Mott, 2001 Finding the molecular basis of quantitative traits: successes

915 and pitfalls. Nat. Rev. Genet. 2: 437–445.

916 Garrison, E., and G. Marth, 2012a Haplotype-based variant detection from short-read

917 sequencing.

918 Garrison, E., and G. Marth, 2012b Haplotype-based variant detection from short-read

919 sequencing.

920 Gimble, F. S., and J. Thorner, 1992 Homing of a DNA endonuclease gene by meiotic

921 gene conversion in Saccharomyces cerevisiae. Nature 357: 301–306.

922 Hehir-Kwa, J. Y., T. Marschall, W. P. Kloosterman, L. C. Francioli, J. A. Baaijens *et al.*,

923 2016 A high-quality human reference panel reveals the complexity and distribution

924 of genomic structural variants. Nat. Commun. 7: 12989.

925 Huang, X., M.-J. Paulo, M. Boer, S. Effgen, P. Keizer *et al.*, 2011 Analysis of natural

926 allelic variation in Arabidopsis using a multiparent recombinant inbred line

927 population. Proc. Natl. Acad. Sci. U. S. A. 108: 4488.

928 Kane, P. M., 2007 The long physiological reach of the yeast vacuolar H+-ATPase. J.

929 Bioenerg. Biomembr. 39: 415–421.

930 Kessner, D., T. L. Turner, and J. Novembre, 2013 Maximum Likelihood Estimation of

931 Frequencies of Known Haplotypes from Pooled Sequence Data. Mol. Biol. Evol. 30:

932 1145–1158.

933 King, E. G., S. J. Macdonald, and A. D. Long, 2012a Properties and power of the

934 Drosophila Synthetic Population Resource for the routine dissection of complex

935 traits. Genetics 191: 935–49.

936 King, E. G., C. M. Merkes, C. L. McNeil, S. R. Hoofer, S. Sen *et al.*, 2012b Genetic

937 dissection of a model complex trait using the Drosophila Synthetic Population

938 Resource. Genome Res. 22: 1558–66.

939 de Koning, D.-J., and L. M. McIntyre, 2017 Back to the Future: Multiparent Populations

940 Provide the Key to Unlocking the Genetic Basis of Complex Traits. Genetics 206:

941 527–529.

942 Koren, S., B. P. Walenz, K. Berlin, J. R. Miller, N. H. Bergman *et al.*, 2017 Canu:

943 scalable and accurate long-read assembly via adaptive k-mer weighting and repeat

944 separation. Genome Res. 27: 722–736.

945 Kover, P. X., W. Valdar, J. Trakalo, N. Scarcelli, I. M. Ehrenreich *et al.*, 2009 A

946 Multiparent Advanced Generation Inter-Cross to Fine-Map Quantitative Traits in

947 Arabidopsis thaliana (R. Mauricio, Ed.). PLoS Genet. 5: e1000551.

948 Kowalec, P., M. Grynberg, B. Pajak, A. Socha, K. Winiarska *et al.*, 2015a Newly

949 identified protein Imi1 affects mitochondrial integrity and glutathione homeostasis in

950 Saccharomyces cerevisiae. FEMS Yeast Res. 15:.

951 Kowalec, P., M. Grynberg, B. Pająk, A. Socha, K. Winiarska *et al.*, 2015b Newly
952 identified protein Imi1 affects mitochondrial integrity and glutathione homeostasis in
953 *Saccharomyces cerevisiae* (I. Dawes, Ed.). FEMS Yeast Res. 15: fov048.

954 Lander, E. S., and D. Botstein, 1989 Mapping mendelian factors underlying quantitative
955 traits using RFLP linkage maps. Genetics 121: 185–99.

956 Lang, G. I., D. Botstein, and M. M. Desai, 2011 Genetic variation and the fate of
957 beneficial mutations in asexual populations. Genetics 188: 647–661.

958 Langmead, B., and S. L. Salzberg, 2012 Fast gapped-read alignment with Bowtie 2.
959 Nat. Methods 9: 357–359.

960 Li, H., 2011 A statistical framework for SNP calling, mutation discovery, association
961 mapping and population genetical parameter estimation from sequencing data.
962 Bioinformatics 27: 2987–2993.

963 Li, H., 2013 Aligning sequence reads, clone sequences and assembly contigs with
964 BWA-MEM.

965 Li, H., and R. Durbin, 2009 Fast and accurate short read alignment with Burrows-
966 Wheeler transform. Bioinformatics 25: 1754–1760.

967 Li, H., B. Handsaker, A. Wysoker, T. Fennell, J. Ruan *et al.*, 2009 The Sequence
968 Alignment/Map format and SAMtools. Bioinformatics 25: 2078–2079.

969 Liti, G., and E. J. Louis, 2012 Advances in quantitative trait analysis in yeast. PLoS
970 Genet. 8: e1002912.

971 Long, Q., D. C. Jeffares, Q. Zhang, K. Ye, V. Nizhynska *et al.*, 2011 PoolHap: Inferring
972 Haplotype Frequencies from Pooled Samples by Next Generation Sequencing (T.

973 Mailund, Ed.). PLoS One 6: e15292.

974 Long, A. D., S. J. Macdonald, and E. G. King, 2014 Dissecting complex traits using the
975 Drosophila Synthetic Population Resource. Trends Genet. 30: 488–495.

976 Macdonald, S. J., and A. D. Long, 2007 Joint estimates of quantitative trait locus effect
977 and frequency using synthetic recombinant populations of Drosophila
978 melanogaster. Genetics 176: 1261–81.

979 Mackay, T. F., 2001 The genetic architecture of quantitative traits. Annu Rev Genet 35:
980 303–339.

981 Manolio, T. A., F. S. Collins, N. J. Cox, D. B. Goldstein, L. A. Hindorff *et al.*, 2009
982 Finding the missing heritability of complex diseases. Nature 461: 747–753.

983 Marçais, G., A. L. Delcher, A. M. Phillippy, R. Coston, S. L. Salzberg *et al.*, 2018
984 MUMmer4: A fast and versatile genome alignment system (A. E. Darling, Ed.).
985 PLOS Comput. Biol. 14: e1005944.

986 Märtens, K., J. Hallin, J. Warringer, G. Liti, and L. Parts, 2016 Predicting quantitative
987 traits from genome and phenome with near perfect accuracy. Nat. Commun. 7:
988 11512.

989 McDonald, M. J., D. P. Rice, and M. M. Desai, 2016 Sex speeds adaptation by altering
990 the dynamics of molecular evolution. Nature 531: 233–236.

991 McMullen, M. D., S. Kresovich, H. S. Villeda, P. Bradbury, H. Li *et al.*, 2009 Genetic
992 properties of the maize nested association mapping population. Science 325: 737–
993 40.

994 Meersche, K. Van den, K. Soetaert, and D. Van Oevelen, 2009 xsample() : An R
995 Function for Sampling Linear Inverse Problems . J. Stat. Softw. 30:.

Mott, R., C. J. Talbot, M. G. Turri, A. C. Collins, and J. Flint, 2000 A method for fine mapping quantitative trait loci in outbred animal stocks. Proc. Natl. Acad. Sci. U. S. A. 97: 12649–54.

Narasimhan, V., P. Danecek, A. Scally, Y. Xue, C. Tyler-Smith *et al.*, 2016 BCFtools/RoH: A hidden Markov model approach for detecting autozygosity from next-generation sequencing data. Bioinformatics 32: 1749–1751.

Navarro-Aviño, J. P., R. Prasad, V. J. Miralles, R. M. Benito, and R. Serrano, 1999 A proposal for nomenclature of aldehyde dehydrogenases in Saccharomyces cerevisiae and characterization of the stress-inducible ALD2 and ALD3 genes. Yeast 15: 829–842.

Noble, L. M., M. V. Rockman, and H. Teotónio, 2019 Gene-level quantitative trait mapping in an expanded C. elegans multiparent experimental evolution panel. bioRxiv 589432.

O'Rourke, S. M., and I. Herskowitz, 2002 A Third Osmosensing Branch in Saccharomyces cerevisiae Requires the Msb2 Protein and Functions in Parallel with the Sho1 Branch. Mol. Cell. Biol. 22: 4739–4749.

Parts, L., F. A. Cubillos, J. Warringer, K. Jain, F. Salinas *et al.*, 2011 Revealing the genetic structure of a trait by sequencing a population under selection. Genome Res 21: 1131–1138.

Paten, B., M. Diekhans, D. Earl, J. S. John, J. Ma *et al.*, 2011a Cactus graphs for genome comparisons, pp. 469–481 in *Journal of Computational Biology*,.

Paten, B., D. Earl, N. Nguyen, M. Diekhans, D. Zerbino *et al.*, 2011b Cactus: Algorithms for genome multiple sequence alignment. Genome Res. 21: 1512–1528.

1019 Pritchard, J. K., 2001 Are Rare Variants Responsible for Susceptibility to Complex
1020 Diseases? Am. J. Hum. Genet. 69: 124–137.
1021 Ruckenstuhl, C., C. Netzberger, I. Entfellner, D. Carmona-Gutierrez, T. Kickenweiz *et*
1022 *al.*, 2014 Lifespan Extension by Methionine Restriction Requires Autophagy-
1023 Dependent Vacuolar Acidification. PLoS Genet. 10:.
1024 Sebastiani, P., N. Solovieff, A. Puca, S. W. Hartley, E. Melista *et al.*, 2011 Retraction.
1025 Science 333: 404.
1026 Solares, E. A., M. Chakraborty, D. E. Miller, S. Kalsow, K. Hall *et al.*, 2018 Rapid Low-
1027 Cost Assembly of the Drosophila melanogaster Reference Genome Using Low-
1028 Coverage, Long-Read Sequencing. G3 (Bethesda). 8: 3143–3154.
1029 Spencer, C. C. A., Z. Su, P. Donnelly, and J. Marchini, 2009 Designing Genome-Wide
1030 Association Studies: Sample Size, Power, Imputation, and the Choice of
1031 Genotyping Chip (J. D. Storey, Ed.). PLoS Genet. 5: e1000477.
1032 Tan, A., G. R. Abecasis, and H. M. Kang, 2015 Unified representation of genetic
1033 variants. Bioinformatics 31: 2202–2204.
1034 The Collaborative Cross, a community resource for the genetic analysis of complex
1035 traits, 2004 Nat. Genet. 36: 1133–1137.
1036 Thornton, K. R., A. J. Foran, and A. D. Long, 2013 Properties and Modeling of GWAS
1037 when Complex Disease Risk Is Due to Non-Complementing, Deleterious Mutations
1038 in Genes of Large Effect (J. K. Pritchard, Ed.). PLoS Genet. 9: e1003258.
1039 Threadgill, D. W., and G. A. Churchill, 2012 Ten years of the Collaborative Cross.
1040 Genetics 190: 291–4.
1041 Tkach, J. M., A. Yimit, A. Y. Lee, M. Riffle, M. Costanzo *et al.*, 2012 Dissecting DNA

damage response pathways by analysing protein localization and abundance changes during DNA replication stress. Nat. Cell Biol. 14: 966–976.

Visscher, P. M., 2008 Sizing up human height variation. Nat. Genet. 40: 489–490.

Walker, B. J., T. Abeel, T. Shea, M. Priest, A. Abouelliel *et al.*, 2014 Pilon: An Integrated Tool for Comprehensive Microbial Variant Detection and Genome Assembly Improvement (J. Wang, Ed.). PLoS One 9: e112963.

Waterhouse, R. M., M. Seppey, F. A. Simão, M. Manni, P. Ioannidis *et al.*, 2018 BUSCO Applications from Quality Assessments to Gene Prediction and Phylogenomics. Mol. Biol. Evol. 35: 543–548.

Wilkening, S., G. Lin, E. S. Fritsch, M. M. Tekkedil, S. Anders *et al.*, 2014 An evaluation of high-throughput approaches to QTL mapping in Saccharomyces cerevisiae. Genetics 196: 853–865.

WTCCC, 2007 Genome-wide association study of 14,000 cases of seven common diseases and 3,000 shared controls. Nature 447: 661–678.

Ye, C., C. M. Hill, S. Wu, J. Ruan, and Z. Ma, 2016 DBG2OLC: Efficient Assembly of Large Genomes Using Long Erroneous Reads of the Third Generation Sequencing Technologies. Sci. Rep. 6: 31900.

Yue, J.-X., J. Li, L. Aigrain, J. Hallin, K. Persson *et al.*, 2017 Contrasting evolutionary genome dynamics between domesticated and wild yeasts. Nat. Genet. 49: 913–924.

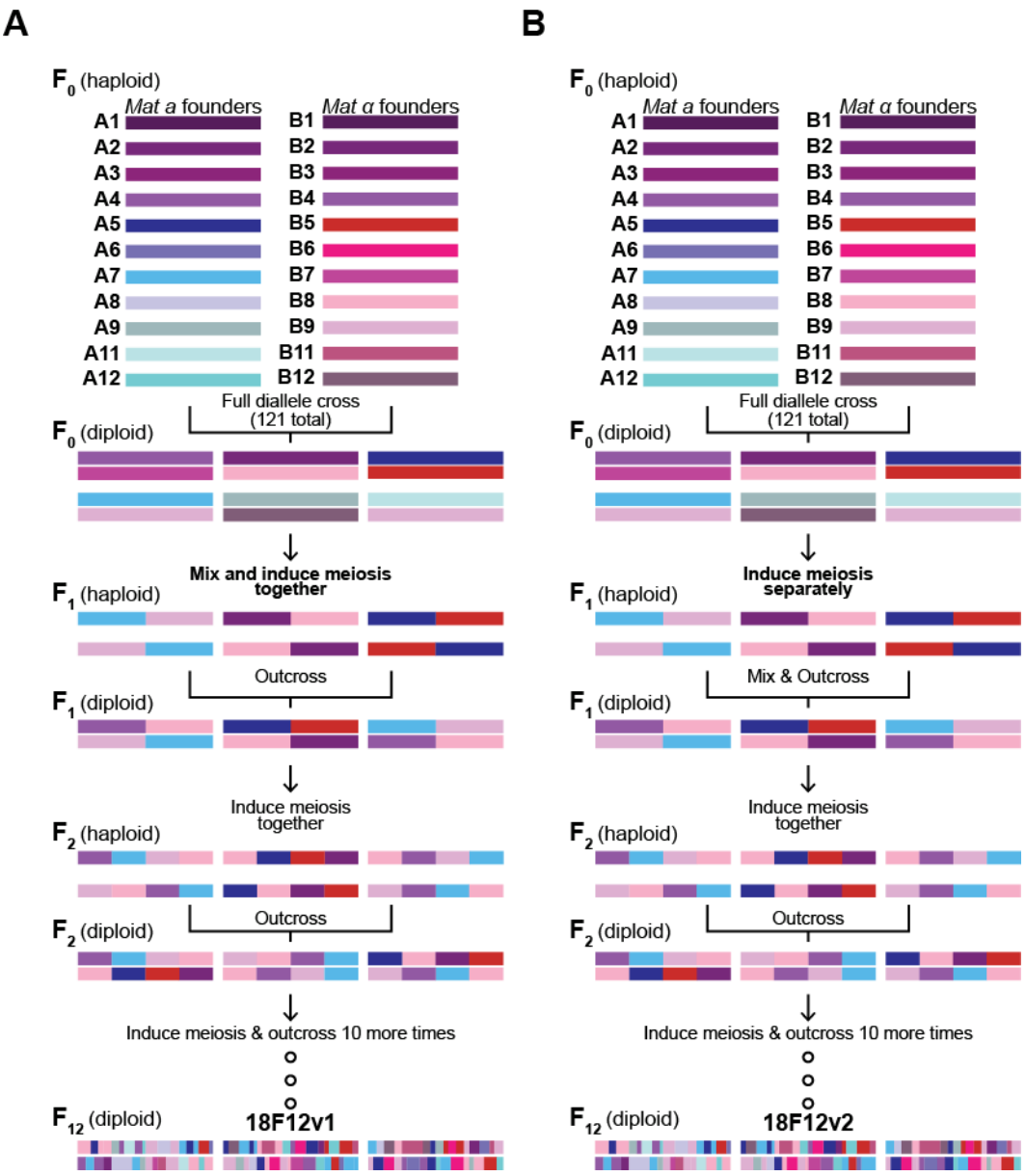

Figure 1. Schematic of the outcrossing process used to make the two 18F12 diploid populations. Both populations were established by a full diallele cross of all 22 isogenic haploid founder strains. A1/B1, A2/B2, A3/B3, and A4/B4 are different mating types of the same strains and are the same strains used in (Cubillos *et al.* 2013). In (**A**), all pairwise crosses were mixed before the first round of sporulation. This is in contrast to (**B**), in which mixing did not occur until after an initial sporulation event. In both cases,

mixed populations were taken through additional rounds of sporulation and random mating for a total of 12 meiotic generations.

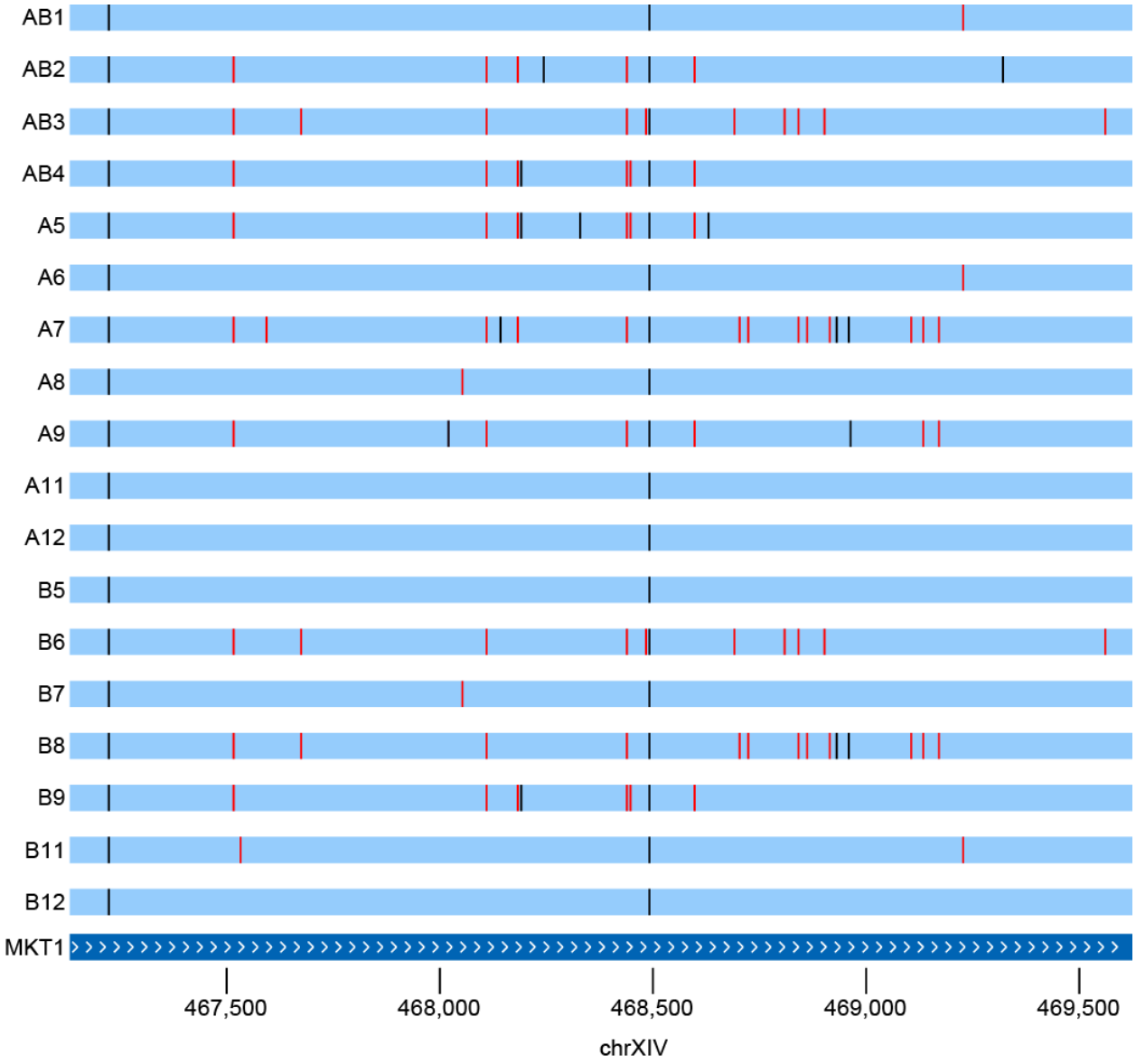

Figure 2. Many alleles of the highly pleiotropic *MKT1* gene are segregating amongst the founder strains, highlighting the potential of uncovering complex allelic series using populations derived from these strains. Seven of these alleles are differentiated by nonsynonymous SNPs, of which six are predicted to be segregating in 18F12v2. Vertical red lines are synonymous SNP differences from the reference S288C strain, and black bars nonsynonymous SNPs.

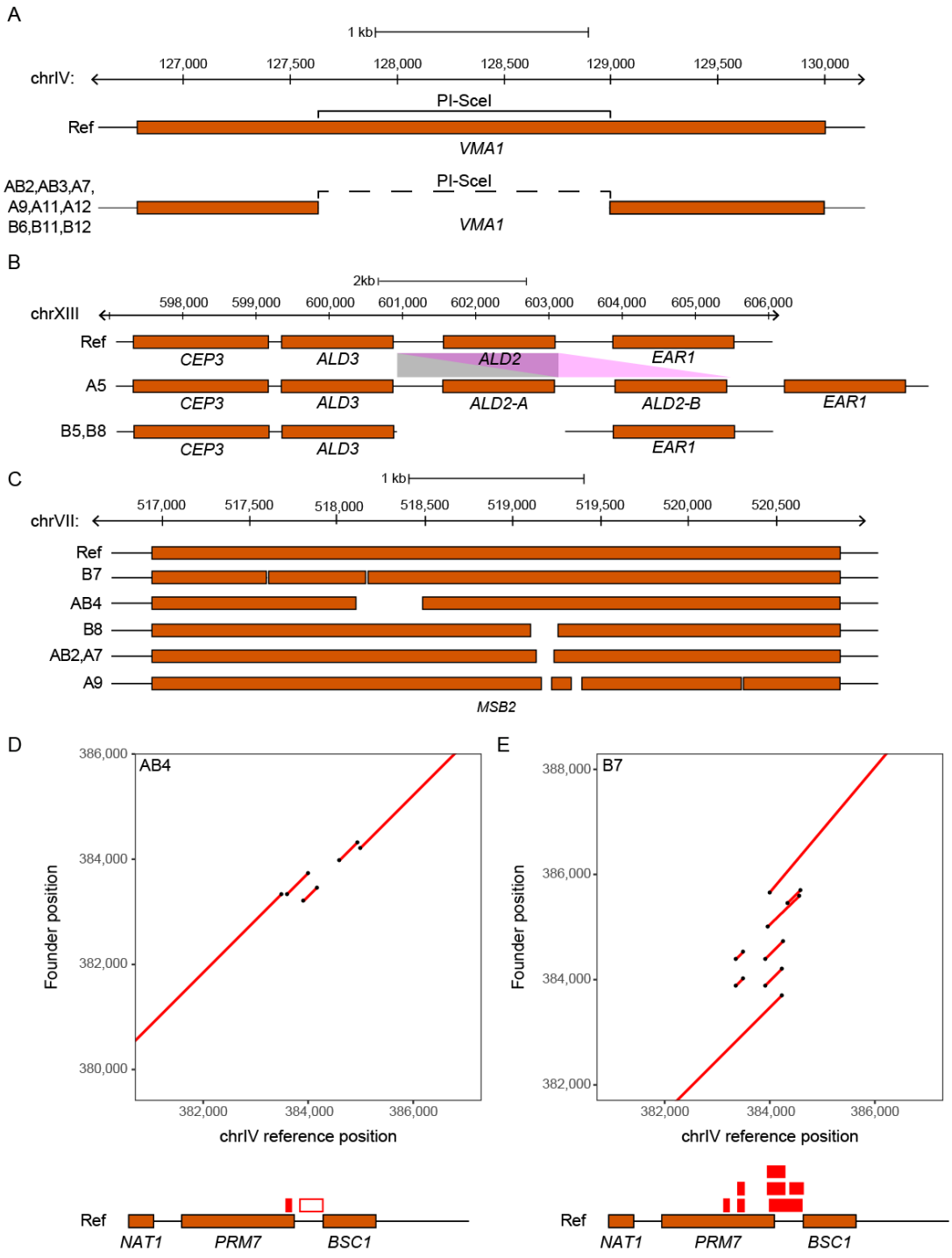

Figure 3. Combining contiguous long-read sequencing with accurate short-read data enables the detection of structural variants such as those depicted above. In (**A**), a large (>1kb) deletion within a vacuolar ATPase (*VMA1*) is present in half of the strains used in this study. This deletion directly overlaps the self-splicing intein, PI-SceI. Copy number

variants of *ALD2*, an aldehyde dehydrogenase, were detected (**B**) and include a duplication of this gene in founder A5 (represented as *ALD2-A* and *ALD2-B*) as well as its' deletion in founders B5 and B8. In (**C**), multiple deletions of different lengths in the osmosensor *MSB2* were detected in multiple founder strains. Dotplots of a structurally complex region on Chromosome IV are shown for founders AB4 (**D**) and B7 (**E**). These plots show alignments of regions from the founder strains (depicted on the y axis) with the corresponding region from the S288C reference strain (depicted on the x axis). The red boxes present above the genes in the reference strain map duplications (solid boxes) and deletions (empty boxes) detected in each founder strain to the corresponding reference sequence. In all panels, the reference strain S288C (aka 'Ref') is used to highlight the various arrangements of SVs present in the founder strains.

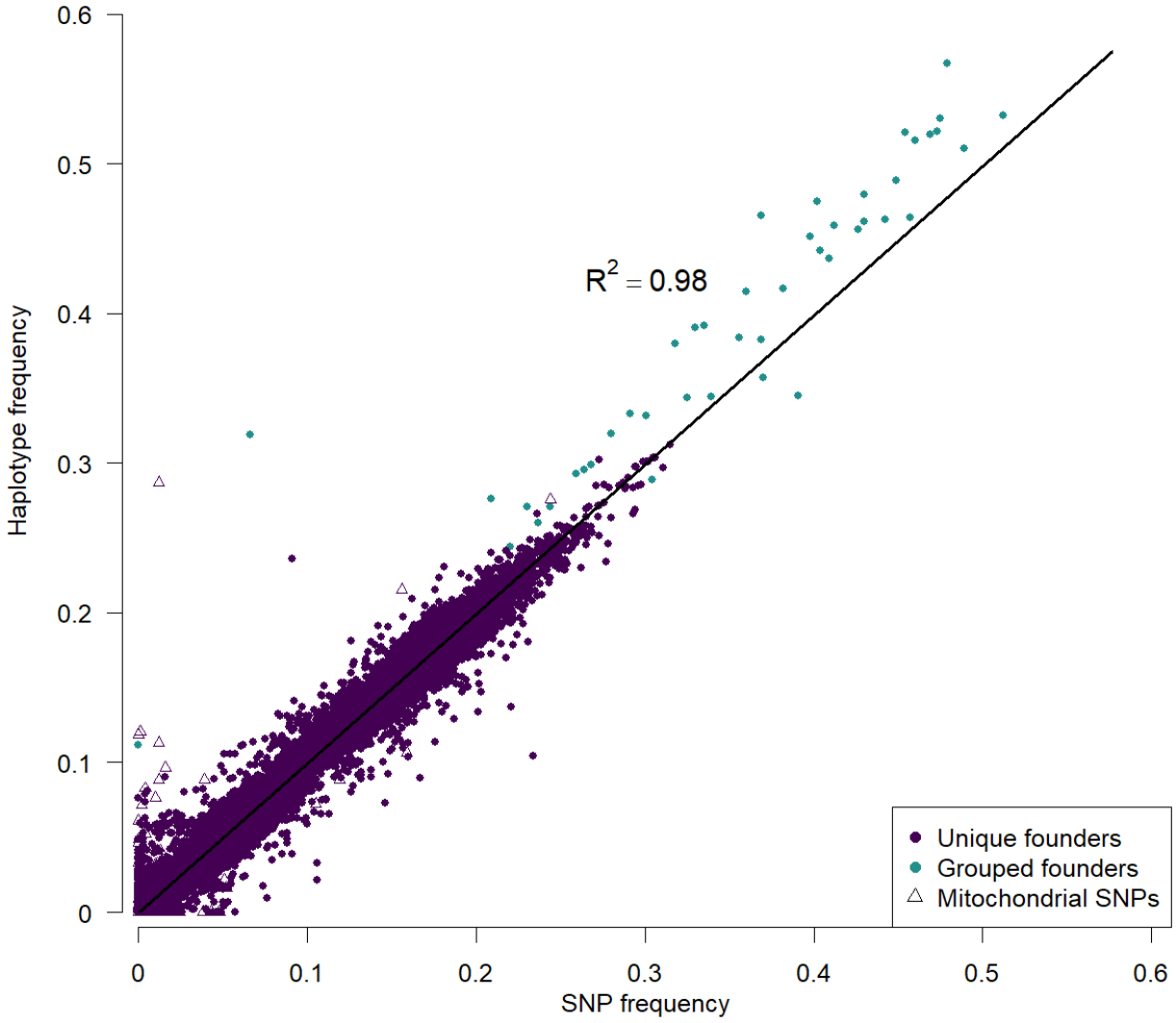

Figure 4. The frequency of SNPs private to a single founder are highly correlated with the estimated haplotype frequencies at these SNPs in 18F12v2. As the frequency of a private SNP should be equal to the corresponding haplotype frequency, this measure provides a benchmark with which the accuracy of our haplotype caller can be measured. Cyan points represent founders that were pooled when estimating haplotype frequencies ("grouped founder") due to the high degree of sequence similarity between

1113 their genomes. Triangles represent mitochondrial SNPs, which, together with SNPs
1114 private to pooled founders, represent the bulk of the major outliers. The coefficient of
1115 determination was calculated by regressing haplotype frequency onto SNP frequency,
1116 excluding SNPs from grouped founders and mitochondrial SNPs.
1117
1118
1119

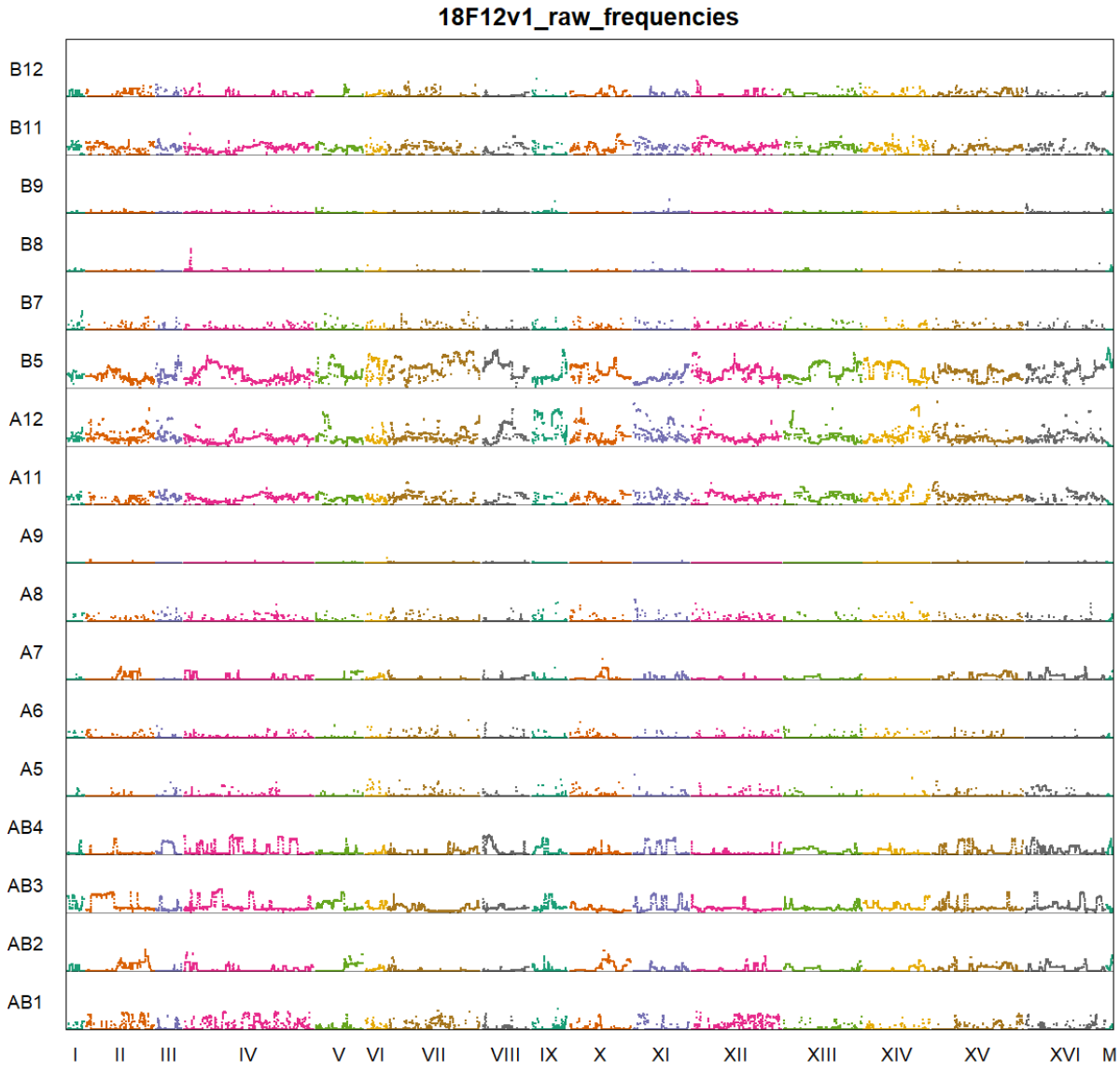

Figure 5. Genome-wide haplotype frequencies for 18F12v1.

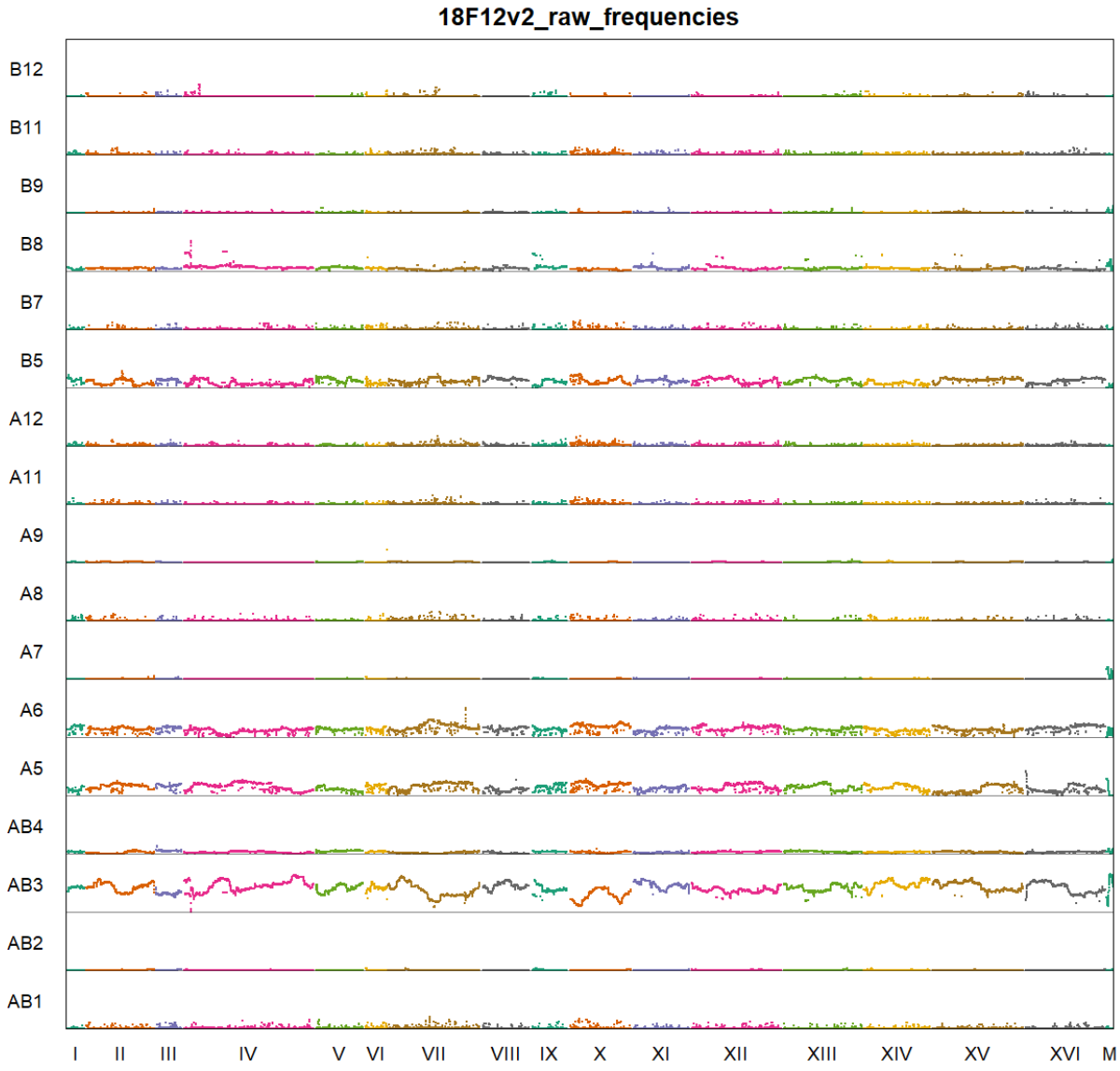

1126

1127 **Figure 6.** Genome-wide haplotype frequencies for 18F12v2.

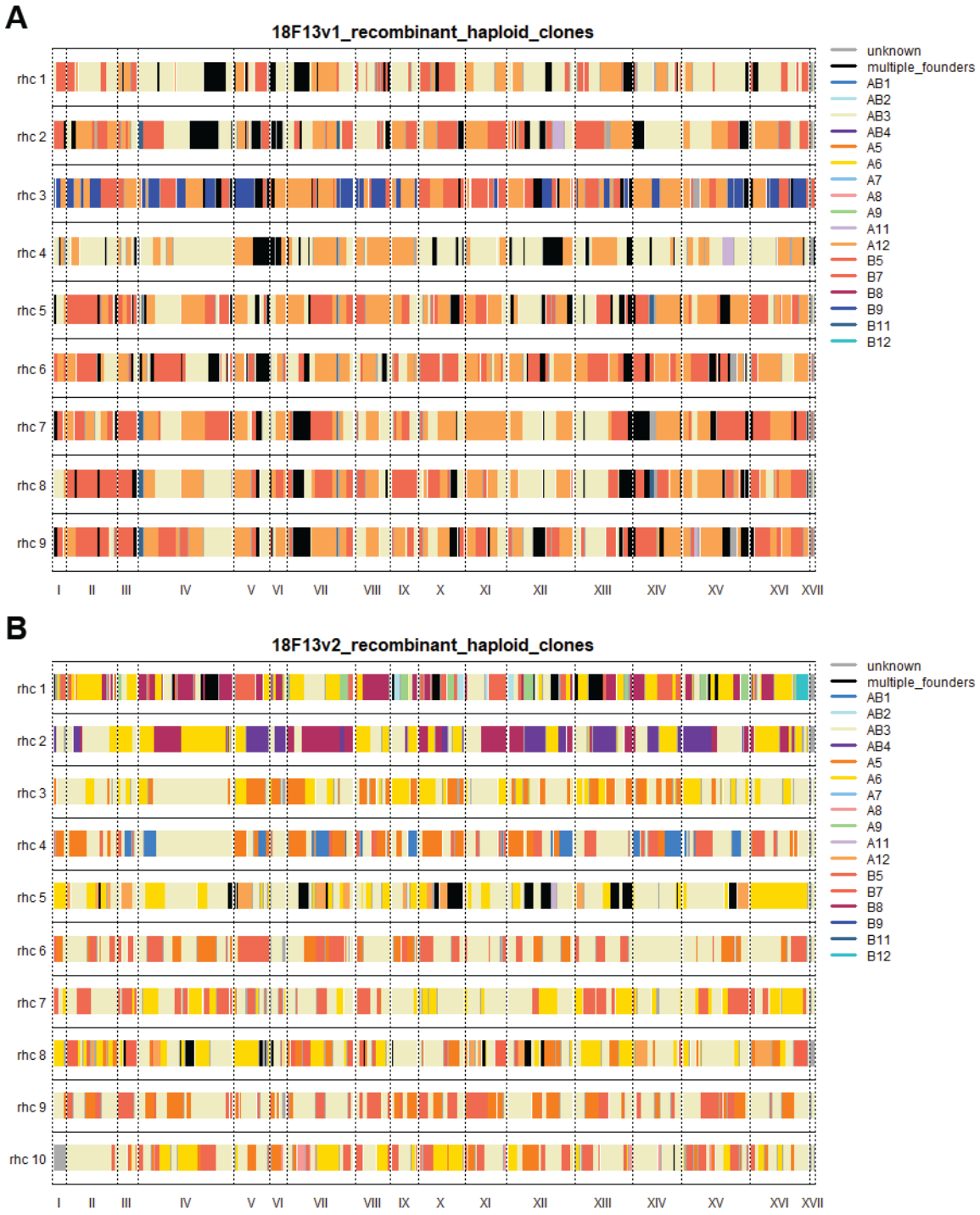

Figure 7. Haploids derived from 18F12v1 (**A**) and 18F12v2 (**B**) were isolated and sequenced, providing a glimpse into the recombinogenic landscape and haplotype diversity present within these populations.

Supplementary Information

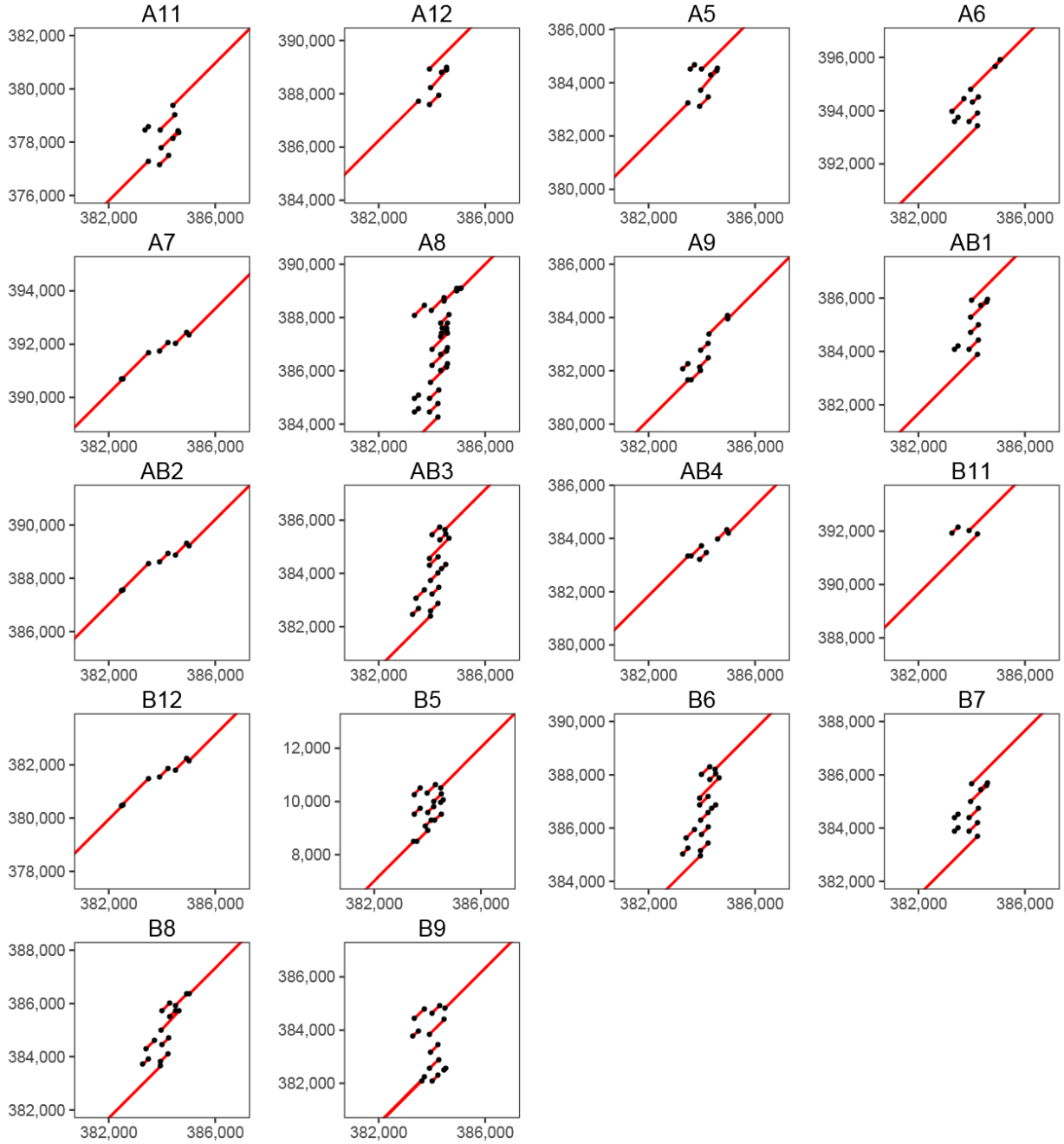

Figure S1. Dot plots showing the numerous structural variants present at this particular site on chromosome IV. Each dot plot was constructed by plotting the sequence alignments of regions from each founder strain (y-axis) against the S288C reference strain (x-axis).

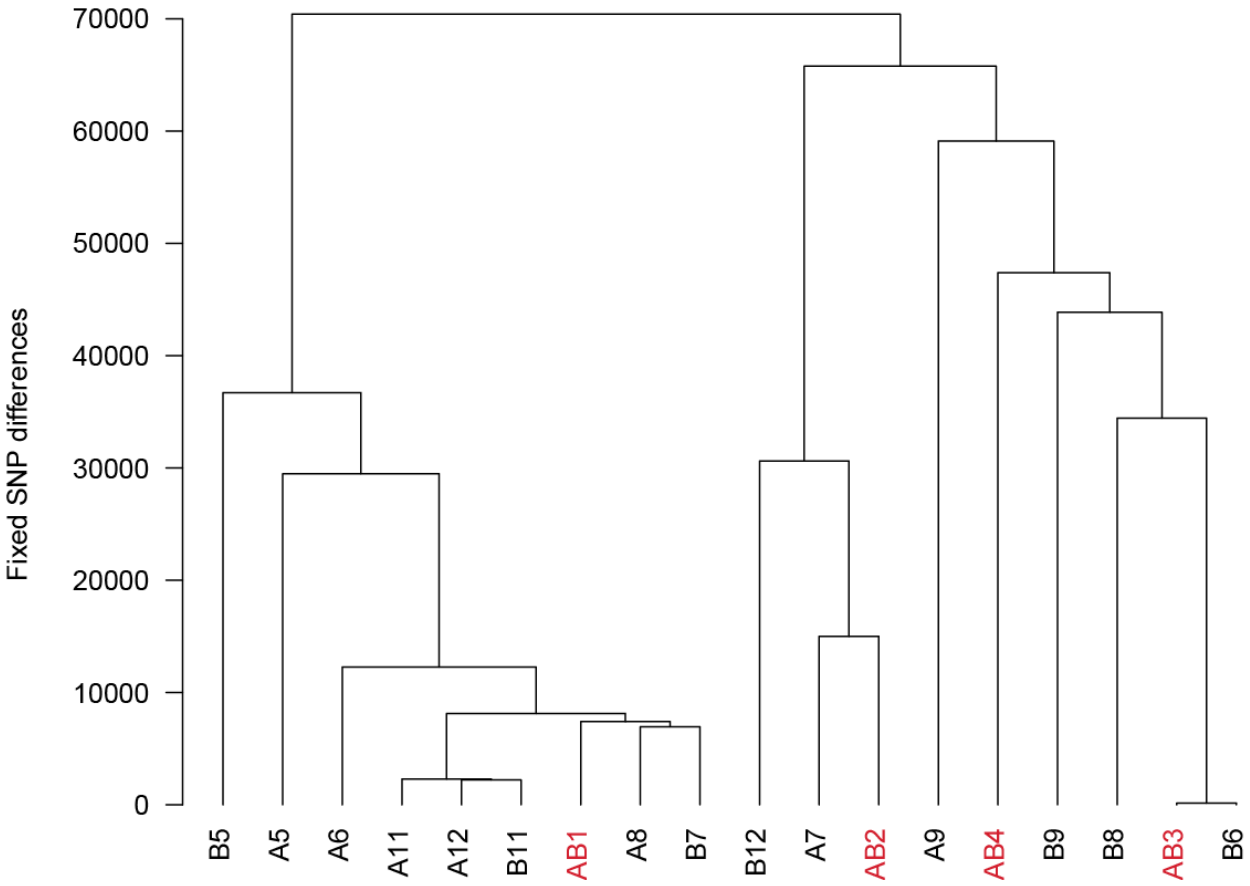

Figure S2. Dendrogram showing the degree of relatedness between the 18 founder strains used in this study. This was constructed in *R* using the *hclust* function on a distance matrix representing the number of differences between each pair of founders. Strains colored in red are the founders from the four-way cross described in Cubillos et al. and used in (Cubillos *et al.* 2013, 2017).

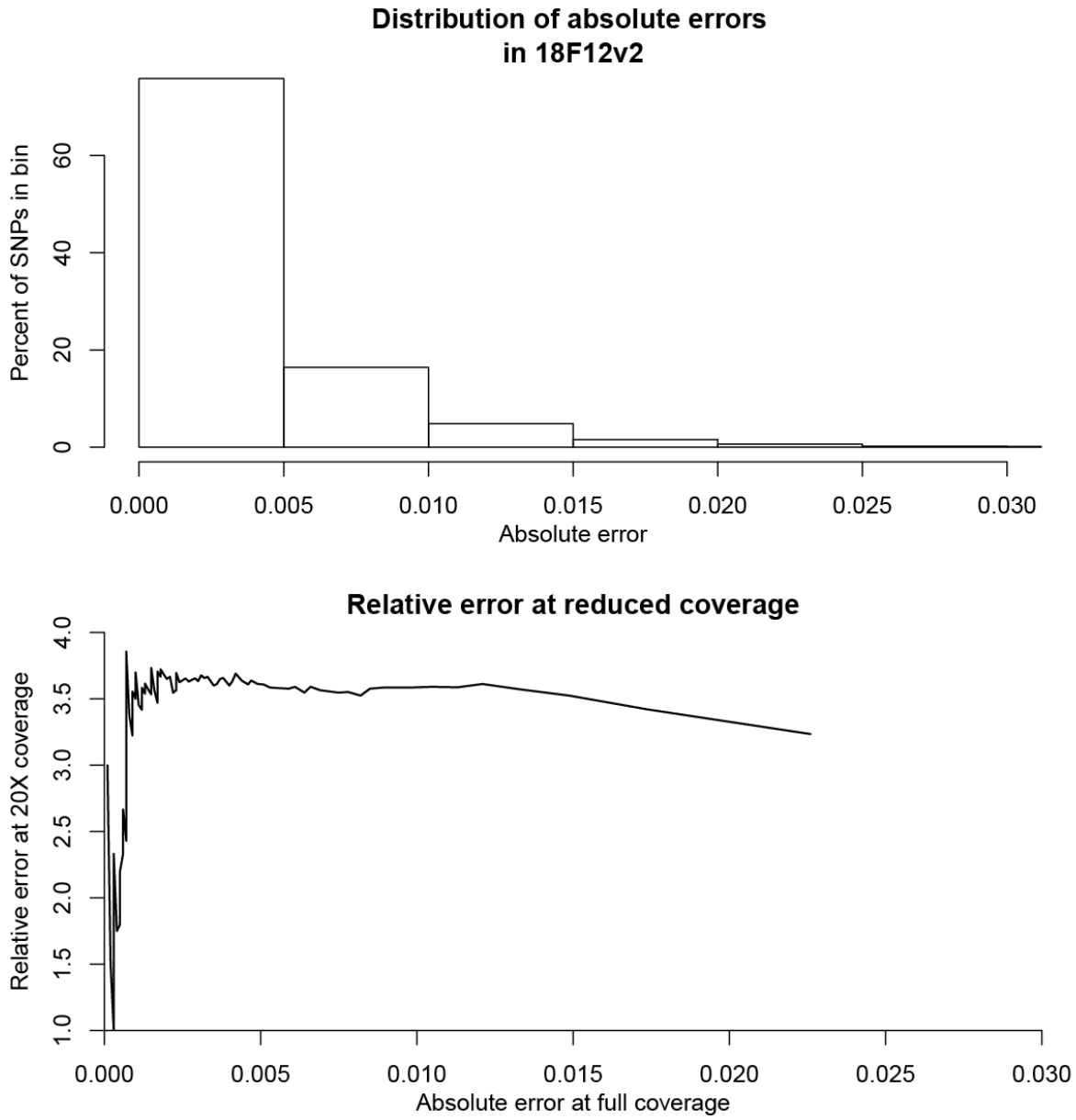

Figure S3. As a measure of the accuracy of the haplotype calling algorithm, we calculated the absolute error between haplotype calls at sites harboring private SNPs and the SNP frequencies in 18F12v2 estimated from 2230X coverage (**A**). The vast majority of sites tested in this manner showed an error rate of less than one percent. We also computed the relative error following downsampling the 18F12v2 data to approximately 20x coverage as a function of the absolute error at full coverage (**B**). At 20X coverage haplotype frequencies are estimated much more accurately than SNP frequencies could be directly estimated at 20X coverage based on binomial sampling.

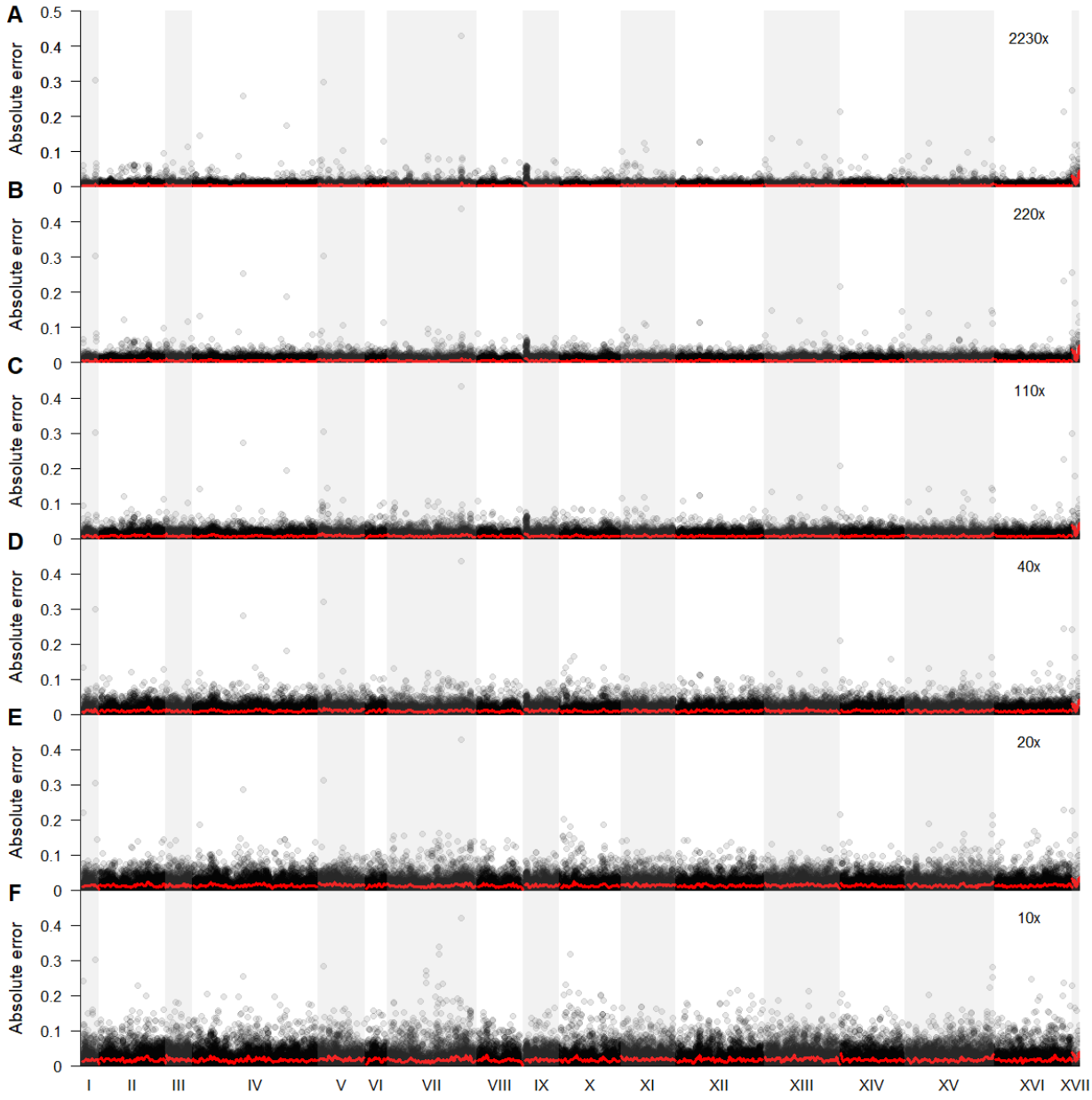

Figure S4. Shown is the absolute error rate between haplotype and SNP frequencies at sites with private SNPs for 18F12v2. Panels A-F represent 100%, 10%, 5%, 2%, 1%, and 0.5% of the full dataset, which approximately corresponds to the coverages shown in the upper right of each panel. The red line represents a kernel regression run using the ksmooth() function in R with kernel set at 'normal' and bandwidth set at 20000, approximating the local expected error rate. Despite clear outliers (that occur irrespective of coverage), haplotype frequency estimates are accurate on average.

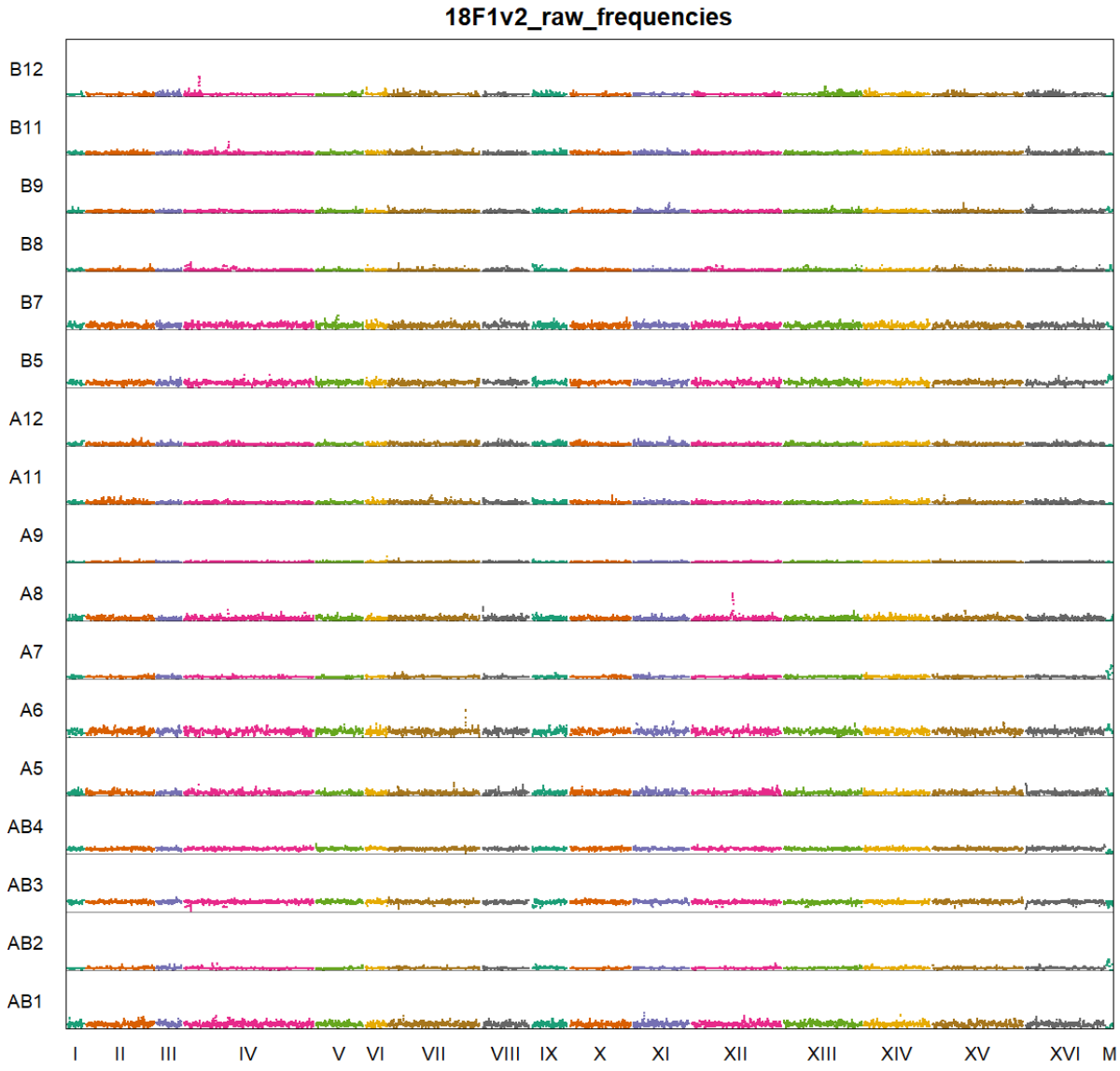

Figure S5. Haplotype frequencies genome-wide for 18F1v2. This sample was taken after the first meiotic generation of version two of the outcrossed population and shows a more balanced distribution of founder haplotypes than the final generation. Haplotype calls for founder B6 were merged with founder AB3, while founders A12 and B11 were merged with founder A11 due their high sequence similarity.

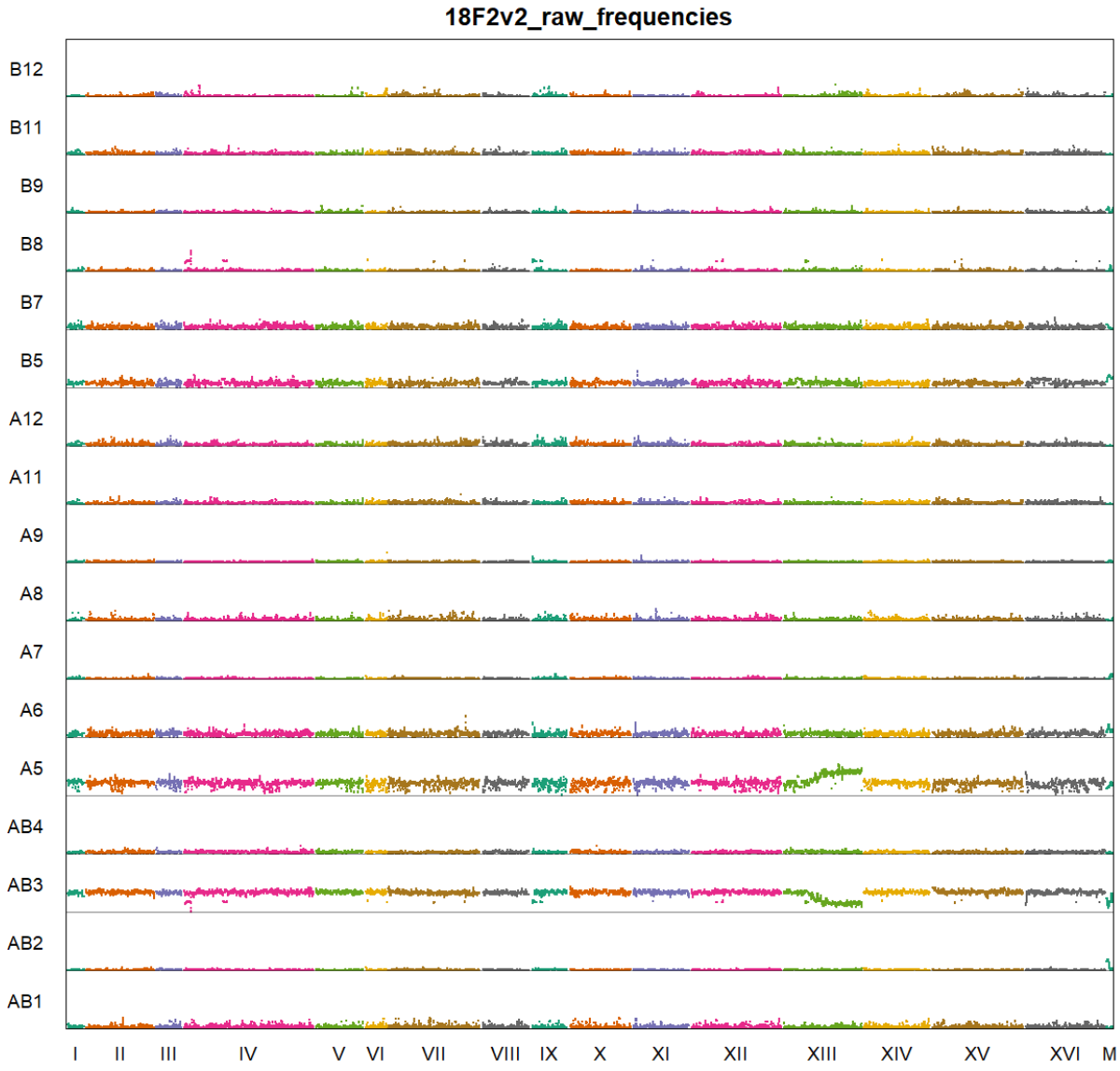

Figure S6. Haplotype frequencies genome-wide for 18F2v2.This sample was taken after the second meiotic generation of version two of the outcrossed population and shows founders AB3 and A5 increasing significantly in frequency as compared to the remaining founders. As above, haplotype calls for founder B6 were merged with founder AB3, while founders A12 and B11 were merged with founder A11.

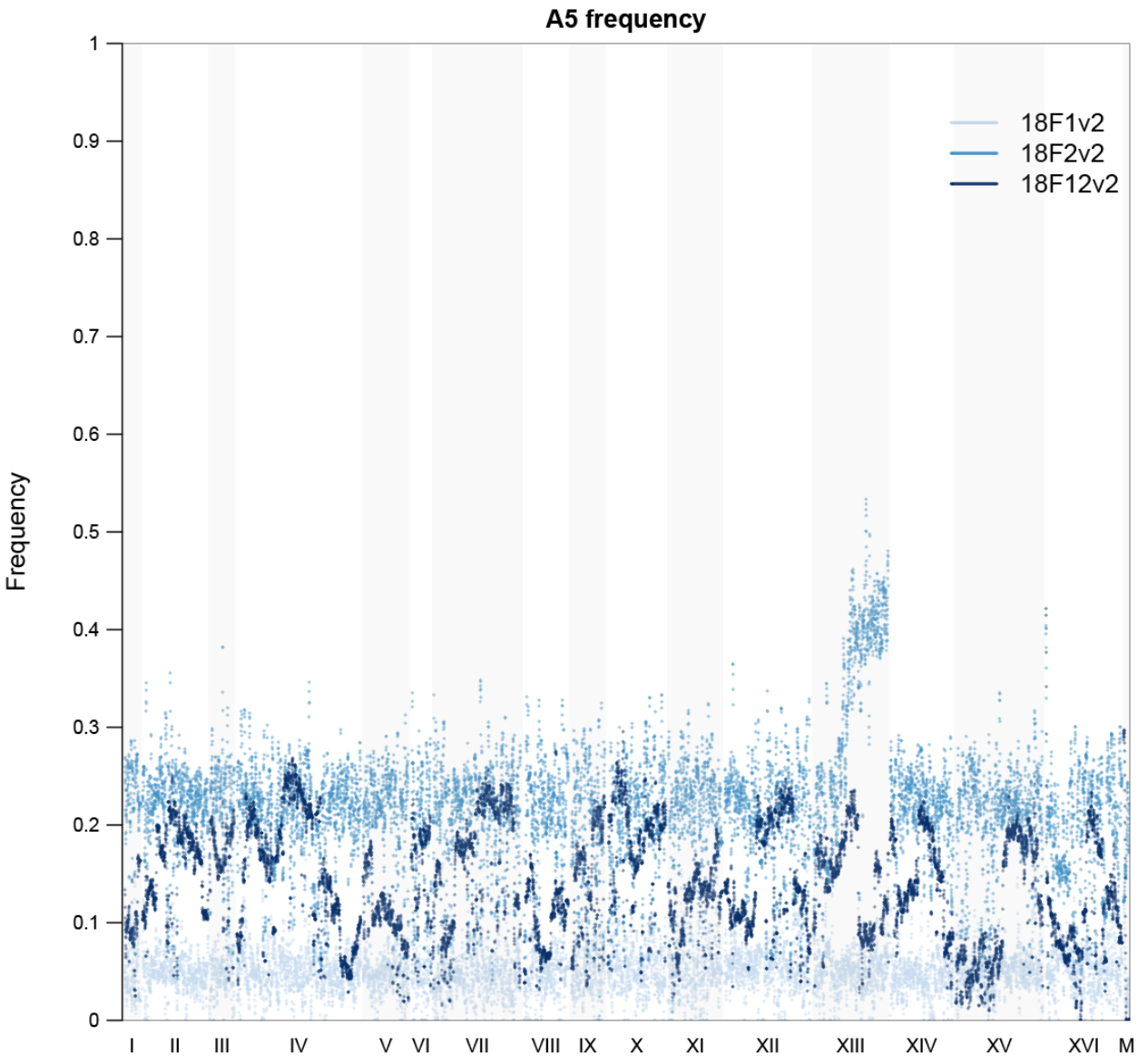

Figure S7. Haplotype frequency genome-wide for the A5 founding strain across the first (18F1v2), second (18F2v2), and twelfth (18F12v2) meiotic generations of the version 2 outcrossed population.

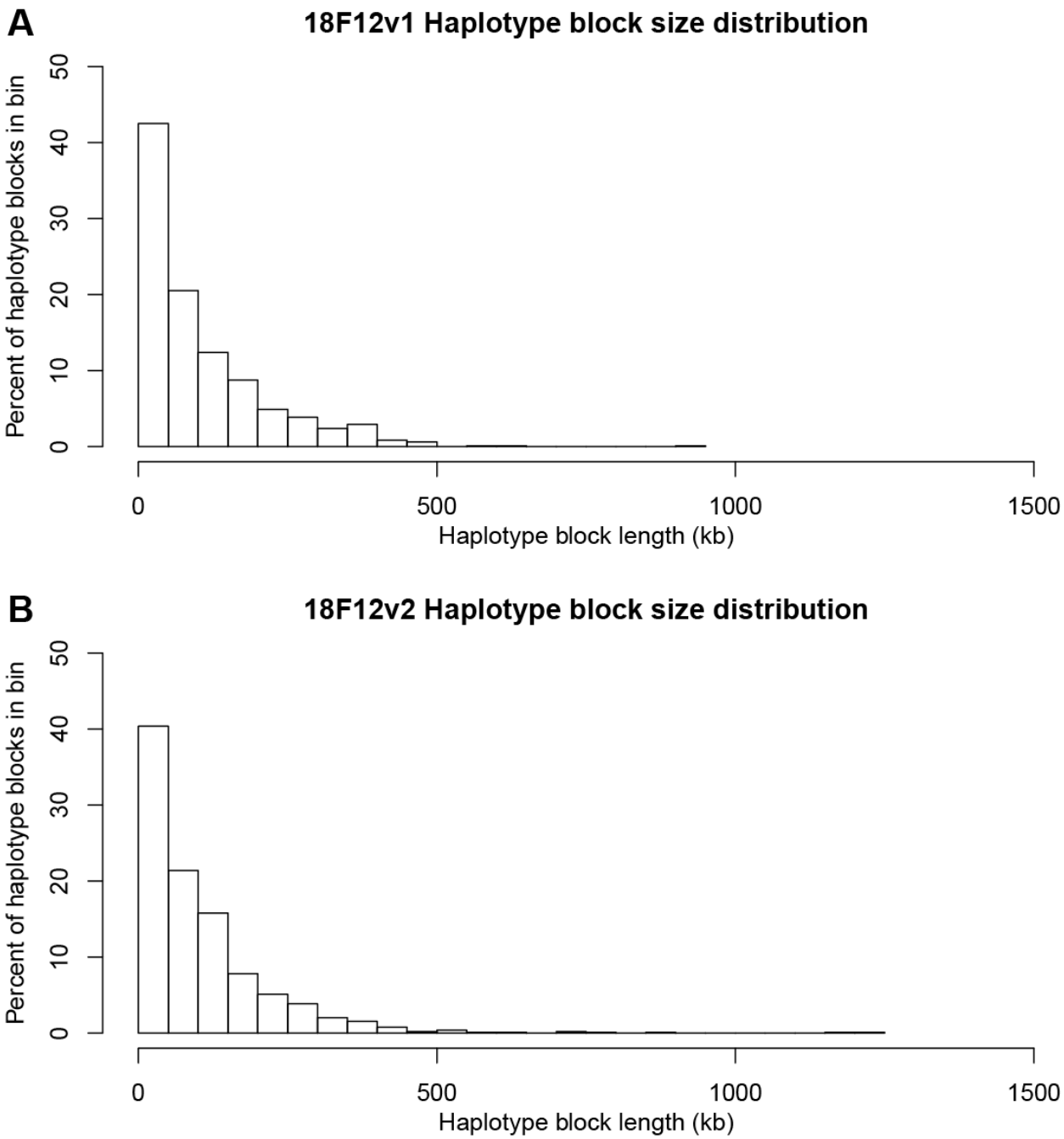

Figure S8. Distribution of haplotype block lengths in recombinant haploid clones derived from 18F12v1 (**A**) and 18F12v2 (**B**). All inferred haplotype blocks, including those called as ties between multiple founding strains, were included in this analysis.

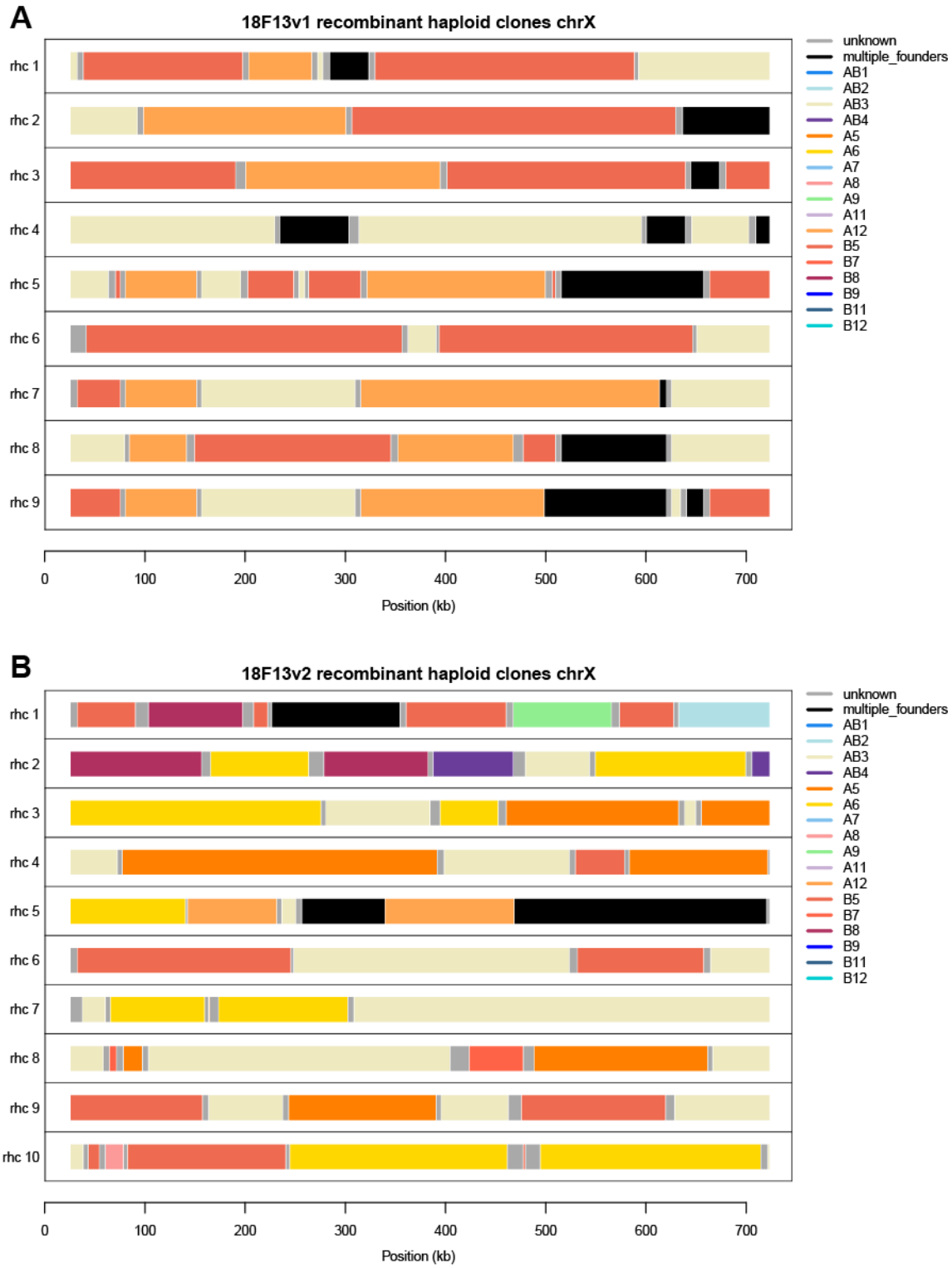

Figure S9. Haplotype diversity at chromosome XII present in 18F13v1 recombinant haploid clones (**A**) and 18F13v2 recombinant haploid clones (**B**).

1220 **Table S1.** List of primers used in this study.

Primer	Sequence (5'-3')	Template	Purpose
pBS_fwd	gcggccgcCCCGGTACCCAGCTTTTG	pBluescript II KS	Assemble *ho*Δ construct
pBS_rev	CGGGGGATCCACTAGTTC	pBluescript II KS	Assemble *ho*Δ construct
HO-US_fwd	tagaactagtggatcccccgTATTCTGATGGCTAACGGTG	Founder B1 gDNA	Assemble *ho*Δ construct
HO-US_rev	gcttcagctgCCTTTAGAGCGCTCCATTTC	Founder B1 gDNA	Assemble *ho*Δ construct
pAG61_fwd	gctctaaaggCAGCTGAAGCTTCGTACG	pAG61	Assemble *ho*Δ construct
pAG61_rev	aaatttttatgATAGGCCACTAGTGGATC	pAG61	Assemble *ho*Δ construct
HO-DS_fwd	agtggcctatCATAAAAATTTCTTGCTTGGC	Founder B1 gDNA	Assemble *ho*Δ construct
HO-DS_rev	aacaaaagctgggtaccggggcggccgcTGCGTTGTTACCACAACTC	Founder B1 gDNA	Assemble *ho*Δ construct
HO-big-flank-F	AAGCGTTCTAAACGCACTATTCA	all hoΔ founder transformants	*ho*Δ check
HO-big-flank-R	ATGGCGTATTTCTACTCCAGCAT	all hoΔ founder transformants	*ho*Δ check
YCR043C-US_MX4_F	TAGAACTAAATGCAAAAGAATATTTGTGCCAAGATAAGGCCAAGAAATTTTTGGGGCAACAGTAGGCAGTGAAAGCGCTCTTAACGTACTTTGGCAAAGGccagctgaagcttcgtacgc	pAG25 (*natMX4*) or pAG32 (*hphMX4*)	*ycr043c*::*natMX4* or *ycr043c*::*hphMX4* deletion
YCR043C-DS_MX4_R	CTCTATGTAGACATATACATATTATTTCATTGCTTTTTGTAATAAACGAGGAAAATGGTGGGATAAAAAAATGCATTGTTATTCCTTCGAAACCAGCAGTgcatagccactagtggatctg	pAG25 (*natMX4*) or pAG32 (*hphMX4*)	*ycr043c*::*natMX4* or *ycr043c*::*hphMX4* deletion
YCR043C-cds-F	agctccacttgatgcttcctta	all *YCR043C* deletion transformants	*YCR043C* deletion check
YCR043C-cds-R	cacctccttccatcttaaagtcg	all *YCR043C* deletion transformants	*YCR043C* deletion check
YCR043C-flank-F	GGCGGGAATGTTGGCTTGGAC	all *YCR043C* deletion transformants	*YCR043C* deletion check/ create larger deletion cassette
YCR043C-flank-R	GCGCTACCGGTAATGCAGTG	all *YCR043C* deletion transformants	*YCR043C* deletion check/ create larger deletion cassette
YCR043C-seq-check-RC	CACTTACCCCTCTGTCAATAGTT	all *YCR043C* deletion transformants	*YCR043C* deletion check via Sanger Sequencing
barcode-check-F	gattcggtaatctccgagcagaag	all founder strains	barcode check
barcode-check-R	ttcagaaacaactctggcgca	all founder strains	barcode check

*Uppercase letters that follow lowercase letters represent the priming sequence, while the lowercase letters represent regions of overlap homology.
**Lowercase letters that follow uppercase letters represent the priming sequence, while the uppercase letters represent regions of flanking homology.

Table S2. Sporulation efficiency of all crosses*

	B1	B2	B3	B4	B5	B6	B7	B8	B9	B11	B12
A1	0	4	1	3	3	4	3	4	4	1	4
A2	2	1	4	1	4	4	4	3	2	1	3
A3	5	3	3	ND**	4	3	4	0	2	4	4
A4	4	4	3	4	3	2	4	4	3	3	4
A5	3	2	3	1	1	2	4	2	0	0	1
A6	3	4	4	3	3	4	4	4	3	2	4
A7	3	4	5	4	4	5	5	5	4	4	5
A8	3	3	3	4	3	2	4	0	4	0	4
A9	5	4	3	3	4	2	4	1	2	4	4
A11	4	4	4	4	4	5	4	3	4	1	4
A12	4	4	4	3	3	3	4	4	4	0	4

*A score of 0 means no asci were visible in the field of view while a score of 5 means approximately 90% or more of the objects in the field of view were asci.

**No data

1300 **Table S3**. Specific sporulation conditions used in this study.

Population	Outcrossing Cycle	Sporulation time (in days)	Sporulation volume (in mL)	Sporulation vessel	Additional notes
18F1v1	1	5	200	1L erlenmeyer	
18F2v1	2	5	200	1L erlenmeyer	
18F3v1	3	5	200	1L erlenmeyer	
18F4v1	4	5	200	1L erlenmeyer	
18F5v1	5	5	200	1L erlenmeyer	
18F6v1	6	5	200	1L erlenmeyer	
18F7v1	7	5	200	1L erlenmeyer	
18F8v1	8	5	200	1L erlenmeyer	
18F9v1	9	5	200	1L erlenmeyer	
18F10v1	10	5	200	1L erlenmeyer	
18F11v1	11	5	200	1L erlenmeyer	
18F12v1	12	5	200	1L erlenmeyer	
18F1v2	1	6	4	24DWP	All crosses sporulated separately
18F2v2	2	4	200	1L erlenmeyer	
18F3v2	3	3	200	1L erlenmeyer	
18F4v2	4	3	50	250mL erlenmeyer	
18F5v2	5	4	50	250mL erlenmeyer	
18F6v2	6	4	50	250mL erlenmeyer	
18F7v2	7	3	50	250mL erlenmeyer	
18F8v2	8	4	50	250mL erlenmeyer	
18F9v2	9	4	50	250mL erlenmeyer	
18F10v2	10	3	50	250mL erlenmeyer	
18F11v2	11	4	50	250mL erlenmeyer	
18F12v2	12	5	50	250mL erlenmeyer	

1301
1302

Table S4. All pairwise SNP differences between founder strains

	AB1	AB2	AB3	AB4	A5	A6	A7	A8	A9
AB1	0	68178	60061	66679	27765	12131	63233	7410	70076
AB2	68178	0	48848	55578	64142	67101	15008	68575	63395
AB3	60061	48848	0	40134	53034	58437	48360	60383	52287
AB4	66679	55578	40134	0	54606	64986	50777	67027	59111
A5	27765	64142	53034	54606	0	29485	59901	27980	66127
A6	12131	67101	58437	64986	29485	0	62410	12281	69433
A7	63233	15008	48360	50777	59901	62410	0	12281	63205
A8	7410	68575	60383	67027	27980	12281	63629	0	70409
A9	70076	63395	52287	59111	66127	69433	63205	70409	0
A11	8140	68612	60416	67088	28220	12261	63669	7898	70395
A12	7988	68533	60365	67049	27943	12154	63594	7794	70361
B5	28183	63545	53668	55176	36714	30476	59484	28362	66654
B6	60023	48876	**157***	40176	53023	58407	48373	60347	52315
B7	7320	68536	60350	66977	27893	12207	63582	6964	70372
B8	58073	52026	34405	44614	54177	56026	51878	58356	53822
B9	54032	56216	43784	47394	49980	53422	54434	54244	57068
B11	8083	68613	60397	67067	28111	12214	63672	7807	70382
B12	45831	25006	52332	59231	49973	46772	30619	46234	65780

	A11	A12	B5	B6	B7	B8	B9	B11	B12
AB1	8140	7988	28183	60023	7320	58073	54032	8083	45831
AB2	68612	68533	63545	48876	68536	52026	56216	68613	25006
AB3	60416	60365	53668	**157***	60350	34405	43784	60397	52332
AB4	67088	67049	55176	40176	66977	44614	47394	67067	59231
A5	28220	27943	36714	53023	27893	54177	49980	28111	49973
A6	12261	12154	30476	58407	12207	56026	53422	12214	46772
A7	63669	63594	59484	48373	63582	51878	54434	63672	30619
A8	7898	7794	28362	60347	6964	58356	54244	7807	46234
A9	70395	70361	66654	52315	70372	53822	57068	70382	65780
A11	0	**2283***	28464	60394	7989	58473	54447	**2294***	46503
A12	**2283***	0	28328	60343	7885	58408	54405	**2217***	46396
B5	28464	28328	0	53655	28475	54111	52160	28451	49324
B6	60394	60343	53655	0	60315	34439	43783	60375	52328
B7	7989	7885	28475	60315	0	58340	54268	8006	46164
B8	58473	58408	54111	34439	58340	0	43869	58454	54419
B9	54447	54405	52160	43783	54268	43869	0	54438	53416
B11	**2294***	**2217***	28451	60375	8006	58454	54438	0	46520
B12	46503	46396	49324	52328	46164	54419	53416	46520	0

*Cells bolded and filled in with blue represent founders that were collapsed due to high sequence similarity (AB3/B6; A11/A12/B11). The table was split for readability.

Table S5. Mean haplotype frequencies genome-wide through one, two, and twelve rounds of outcrossing in 18F12v2.

Founder	18F1v2_frequency	18F2v2_frequency	18F12v2_frequency
AB1	8.0%	3.2%	1.2%
AB2	4.4%	1.3%	0.5%
AB3	17.6%	33.2%	41.4%
AB4	9.0%	3.3%	3.3%
A5	5.0%	21.8%	14.0%
A6	10.5%	6.4%	14.3%
A7	4.2%	1.2%	0.4%
A8	4.3%	2.2%	0.7%
A9	1.1%	1.4%	0.5%
A11	3.5%	2.8%	1.2%
A12	3.6%	3.4%	1.7%
B5	9.1%	8.4%	11.3%
B7	7.2%	4.6%	1.0%
B8	2.3%	1.4%	5.7%
B9	3.2%	1.3%	0.8%
B11	3.1%	2.6%	1.3%
B12	3.8%	1.4%	0.6%

Note S1. Strains A9, B1, and B9 all grew slowly after O/N incubation, so all 5mL from each culture was transferred to 5mL of YPD and incubated an additional 3h at 30°C at 250 RPM. During this time, the rest of the haploid strains remained at RT. For mating, 200uL of culture from these slow-growing strains was mixed with 100uL of culture from the rest of the haploid strains..

Note S2. Before taking OD630 measurements, the following crosses were accidentally combined: A5xB6 with A5xB7, A6xB2 with A6xB3, A6xB8 with A6xB4, and A11xB7 with A11xB6. To correct for this, twice of much of the combined cultures were added to the final spore pool after normalizing cell density.

Note S3. Founder strains A5, A7-A9, A11, A12 and B5-B12 (excluding B10) were sequenced using PE100 reads, while founders A1-A4 and A6 were sequenced using PE150 reads.

Note S4. In one of the recombinant haploid clones derived from 18F12v2 (rhc 10), the entirety of chromosome I was called as unknown. Closer examination showed that this chromosome is duplicated and heterozygous for two founding strains, suggesting a partial diploidization event.